

NACA RM E55C22

**NACA**

# RESEARCH MEMORANDUM

INJECTION PRINCIPLES FROM COMBUSTION STUDIES

IN A 200-POUND-THRUST ROCKET ENGINE

USING LIQUID OXYGEN AND HEPTANE

By M. F. Heidmann and C. M. Auble

Lewis Flight Propulsion Laboratory  
Cleveland, Ohio

CLASSIFICATION CHANGED  
UNCLASSIFIED

To \_\_\_\_\_

By authority of *NACA Res. Lab. E. Heidmann*  
*4 RN-113* Date *3-19-57*

*NB 4-3-57*

CLASSIFIED DOCUMENT

**RESEARCH MEMORANDUM**  
**JUN 7 1955**  
**LEWIS AERONAUTICAL LABORATORY**  
**CLEVELAND, OHIO**  
**LANGLEY FIELD, VIRGINIA**

This material contains information affecting the National Defense of the United States within the meaning of the espionage laws, Title 18, U.S.C., Secs. 793 and 794; the transmission or revelation of which in any manner to an unauthorized person is prohibited by law.

## NATIONAL ADVISORY COMMITTEE FOR AERONAUTICS

WASHINGTON

June 7, 1955

## NATIONAL ADVISORY COMMITTEE FOR AERONAUTICS

RESEARCH MEMORANDUMINJECTION PRINCIPLES FROM COMBUSTION STUDIES IN A 200-POUND-THRUST  
ROCKET ENGINE USING LIQUID OXYGEN AND HEPTANE

By M. F. Heidmann and C. M. Auble

## SUMMARY

The importance of atomizing and mixing liquid oxygen and heptane was studied in a 200-pound-thrust rocket engine. Ten injector elements were used with both steel and transparent chambers. Characteristic velocity was measured over a range of mixture ratios. Combustion gas-flow and luminosity patterns within the chamber were obtained by photographic methods.

The results show that, for efficient combustion, the propellants should be both atomized and mixed. Heptane atomization controlled the combustion rate to a much larger extent than oxygen atomization. Induced mixing, however, was required to complete combustion in the smallest volume. For stable, high-efficiency combustion and smooth engine starts, mixing after atomization was most promising.

## INTRODUCTION

In rocket engines, complete burning must occur in a small volume. In addition, burning must be free from destructive oscillations and should result in low heat transfer to the chamber walls.

The high mass through-put in rocket engines requires rapid mixing and dispersion of propellants. The extent to which these needs are met depends largely on how the propellants are prepared. Not only must atomization and mixing by the injector be considered, but also turbulence and heat transfer during combustion. At present, the over-all process cannot be theoretically predicted; even the independent action of the injector or combustion is only qualitatively known. Therefore, injector-design data must be obtained from laboratory and engine tests.

The study of injection has been approached in various ways. References 1 to 4 are typical of studies made on sprays and orifice flows. Such studies, however, may not apply to burning conditions. Engine performance has also been reported for some injector designs (refs. 5 and 6). These data have generally been obtained to optimize one injection

scheme. Information gained from sampling probes and by photography has also been reported for many injector designs (refs. 7 to 10). The time required for such detailed studies has limited the scope of these techniques. So far, the reported data on the injector requirements for a specific propellant combination are not complete.

Propellants may be injected in so many ways that it is impractical to test each one separately. All schemes, however, involve atomization and mixing and differ only in the degree in which these functions are performed. Atomization and mixing as characteristic functions are used to describe injectors in the following list, which includes most injectors for a bipropellant system:

- (1) No mixing or atomization
- (2) Atomization without mixing
  - (a) Atomization of oxidant
  - (b) Atomization of fuel
  - (c) Atomization of both propellants
- (3) Mixing without atomization
- (4) Mixing with atomization
  - (a) Mixing before atomization
  - (b) Mixing after atomization

The performance of 10 injectors designed to simulate these processes are presented herein. The program was intended to show the importance of atomization and mixing for the liquid oxygen - heptane propellant combination. Also, a correlation between combustion characteristics and the injection process was desired.

The study was made with a rocket designed for a thrust level of 200 pounds and chamber pressure of 300 pounds per square inch. Results include characteristic velocity, combustion-chamber gas velocity, and motion pictures of combustion showing gas luminosity and flow paths. Stability and starting characteristics were also studied.

## APPARATUS AND PROCEDURE

### Rocket Installation

The rocket engine (fig. 1) consisted of injector, chamber, and convergent nozzle in separable units. Transparent plastic chamber sections replaced steel sections during photographic studies. Chambers 2 inches in diameter and 8 inches long were generally used; the characteristic chamber length  $L^*$  was 51 inches. In some runs, chambers 4 and 2 inches

long were used. Test runs were controlled by a program timer and were of 2- to 3-second duration. A pressurized-tank propellant feed system was used. The oxygen tank was in a liquid nitrogen bath for temperature control.

### Injectors

The basic injection pattern used in this study was that of one fuel jet spaced between two oxidant jets. This pattern varied only in that atomization or mixing was induced. Features of the injectors used to simulate various processes are summarized in table I. A more detailed description, together with water-spray photographs taken at a pressure drop of 100 pounds per square inch, is presented in part (a) of figures 2 to 11. A design pressure drop of 100 pounds per square inch was used at an oxidant-fuel weight ratio  $o/f$  of 2.4. Detailed performance results are also presented in figures 2 to 11 so that injector description and performance may be more readily correlated. This performance is discussed hereinafter.

### Instrumentation

Engine instrumentation was used to record chamber total pressure, propellant flow rate, and propellant temperature. Chamber pressure was measured at the injector face with a 500-pound-per-square-inch Bourdon tube instrument. The probable measurement error was  $\pm 0.4$  percent of full scale. This pressure was compared with the reading of a strain-gage instrument with a probable error of  $\pm 4$  pounds per square inch. Volumetric flow rates were measured with rotating-vane-type meters. The probable error was  $\pm 1$  percent. The temperature of the flowing propellants was measured with thermocouples. The probable errors were  $\pm 3^\circ$  and  $\pm 1^\circ$  F for the oxygen and the fuel, respectively.

Photographic equipment included one 3000-frame-per-second, 16-millimeter camera arranged to record three views of the chamber. A 16-millimeter moving-film camera was used for streak photographs. The camera arrangement is shown in figure 12. Timing marks of 120 cycles per second for the motion-picture camera and 1000 cycles per second for the moving-film camera were exposed on the film.

### Performance Measurements

The performance of characteristic exhaust velocity  $c^*$  was measured at oxidant-fuel weight ratios  $o/f$  from about 1.2 to 3.0 for each injector. Total propellant flow rate was maintained constant at about 0.9 pound per second for each injector and operating condition. The  $c^*$  was calculated from

$$c^* = \frac{P_c A_t g}{w} \quad (1)$$

(Symbols are defined in appendix A.) The probable error in  $c^*$  based on instrument accuracy was  $\pm 2.5$  percent; however, data were generally reproducible within  $\pm 1$  percent. Theoretical equilibrium curves for the liquid oxygen - heptane propellant combination are shown in figure 13. For plastic chamber work, the weight loss in plastic was assumed to be a direct addition to the fuel flow. The rate was assumed constant during a run. Corrections to  $c^*$  were made using this assumption.

Streak photographs were used to determine chamber gas velocities. Typical streak photographs are shown in figure 14. The method of analysis is similar to that reported in references 11 and 12. Several streaks were averaged to determine gas velocity. A value of  $o/f$  between 2.0 and 2.4 was desired for analysis; however, the actual  $o/f$  varied because of the plastic weight-flow addition. The probable error in measured velocity was  $\pm 5$  percent. The velocity measurements at the chamber exit were checked by comparison with a velocity calculated from the experimental  $c^*$ . The relation between these parameters is as follows:

$$(c^*)^2 \gamma \left( \frac{2}{\gamma + 1} \right)^{\frac{\gamma+1}{\gamma-1}} = c^* \frac{A_c V_c}{A_t} - \frac{V_c^2}{2} \quad (2)$$

The derivation of equation (2) is shown in appendix B. A graphical representation of this equation is presented in figure 15.

Gas-flow patterns in the chamber were observed from projected 3000-frame-per-second photographs.

Analyses of instabilities and ignition and starting transients were made on a qualitative basis from photographic evidence.

## RESULTS AND DISCUSSION

Injector description, performance characteristics, combustion photographs, and flow patterns are shown in figures 2 to 11. These data are summarized in table II, and subsequent discussion refers to table II unless otherwise noted.

Performance during stable operation is discussed first. Other performance characteristics are discussed later in this report.

### No Mixing or Atomization

3572

With no mixing or atomization,  $c^*$  efficiency at an  $o/f$  of 2.4 was about 40 percent with the wide jet spacing and 48 percent with close spacing. Both parallel-jet injectors showed similar variation of  $c^*$  with  $o/f$ . A change in jet spacing therefore did not appreciably change performance. The chamber gas velocity, however, was different with each of these injectors. A reverse flow or recirculation near the injector, evident with a wide spacing between jets, disappeared as the spacing was reduced. The gas flow illustrated in the combustion photographs (figs. 2(c) and 3(c)) also indicates this change in flow. Gas velocity near the nozzle also differed for the two injectors. With a wide spacing of jets, gas velocity approached a constant value; whereas, with a close spacing it continued to rise. This indicates that the  $c^*$  comparison may vary with different chamber lengths.

The change in jet spacing appears mainly to affect the initial preparation in the chamber. With close spacing, mixing is better near the injector, and the resulting combustion develops with less large-scale turbulence.

### Atomization Without Mixing

Atomization of oxidant. - The  $c^*$  obtained with atomized oxygen and a fuel jet was about 50 percent of theoretical at an  $o/f$  of 2.4. Compared with that of the wide-space parallel-jet injector, which also had 1/4-inch spacing between fuel and oxidant,  $c^*$  rose only 10 percentage points. Neither did the gas velocities of the two configurations differ greatly. Although no reverse flow was obtained, the profiles of the velocity curves were quite similar. This similarity indicates that better atomization and distribution of oxygen did not permit combustion to proceed much more rapidly. This result may be attributed to the following two causes: (1) The fuel was so poorly prepared that only a small amount of atomized oxygen entered into the reaction; or (2) the oxidant was readily dispersed when injected as a liquid jet. Subsequent comparisons show that the latter is more nearly correct.

Atomization of fuel. - With both fuel-atomizing injectors,  $c^*$  was appreciably higher than with previous injectors, even though the oxygen was injected in jet form. With an atomized fuel sheet, the efficiency at an  $o/f$  of 2.4 was about 70 percent; whereas, with an atomized fuel cone it was about 80 percent. The gas-velocity profiles were quite similar in that velocity increased uniformly. The  $c^*$  probably differed because of the better mixing and fuel distribution with a fuel cone. Water-spray photographs for this injector (fig. 6(a)) show that mixing is quite thorough. Therefore, it may be concluded that the performance of the fuel-sheets injector more closely demonstrates the independent effect of fuel atomization.

Fuel atomization caused an increase in  $c^*$  of about 30 percentage points when compared with wide-spaced parallel jets, in which no atomization or mixing occurred. Also, the gas velocity developed more uniformly and rapidly with fuel atomization. This result shows that the amount of fuel atomized was controlling the rate at which combustion proceeded. It also shows, in view of the result with atomizing the oxygen, that oxygen was reasonably well prepared when injected as a jet. This result may be related to the difference in physical properties of the two propellants.

Atomization of both propellants. - With both propellants atomized, but with little or no induced mixing,  $c^*$  was 82 percent of theoretical at an o/f of 2.4. Gas velocity increased uniformly, given results similar to those obtained with fuel atomization alone. These results emphasize the importance of fuel atomization above that of oxygen atomization. Atomizing the oxygen improved  $c^*$  an average of 11 percentage points, whether fuel was in jet form or in the atomized state. In contrast, atomizing the fuel improved  $c^*$  an average of 31 percentage points, whether oxygen was in jet form or in the atomized state.

#### Mixing Without Atomization

No data were obtained with the premix injector designed to determine the effect of mixing without atomization. Three attempts at running injectors of this type were made, but destruction of the premix chamber occurred in each case. Violent detonations occurred at the start, evidently propagating a reaction into the mixing cavity. Flow conditions appeared normal prior to ignition.

#### Mixing with Atomization

Mixing before atomization. - Experience with the premix injector showed that premixing followed by atomization was not feasible in the study of mixing before atomization. Thus, impinging jets were used to study this condition. Whether or not mixing actually occurred before atomization is not known, but these injectors were considered a practical approach to this condition.

The evaluation of mixing before atomization is incomplete because stable operation was not possible above an o/f of about 2.0. This was true for both impinging-jet injectors. The  $c^*$ , however, appears higher than with no mixing. Estimated efficiencies in the region of maximum theoretical  $c^*$  are 90 and 84 percent for the long-stream-length and surface-impinging injectors, respectively. The efficiency for atomization but no mixing was about 82 percent. Therefore, an increase of as much as 8 percentage points may be obtained by mixing the atomized propellants.

The gas-velocity profile emphasizes the importance of mixing more than does  $c^*$ . With the long-stream-length injector, velocity increased rapidly and reached a maximum value about midway in the chamber. A comparison of gas velocities obtained with and without mixing shows that mixing causes an appreciable increase in combustion rate.

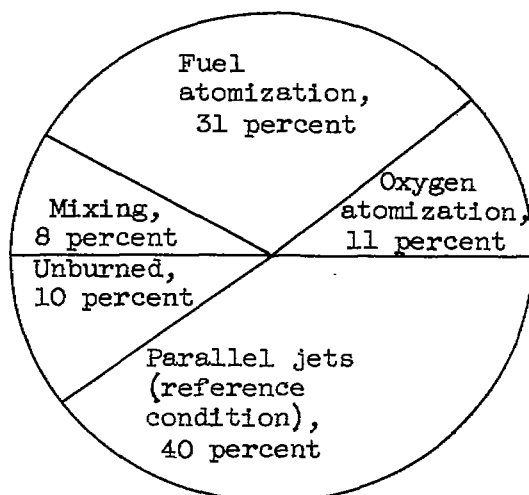
Performance with the surface-impinging (short-stream-length) injector was not as good. The poorer performance may be due to propellants splashing back on the injector face. This splashing would be expected to decrease the atomization effectiveness. High-speed motion pictures of combustion gave this impression, although it was not evident in water-flow tests. Because of these uncertainties, this injector may not be typical of mixing before atomization.

Mixing after atomization. - Mixing propellants after they have been atomized also appears to be effective in increasing combustion rate. A  $c^*$  efficiency of about 87 percent was obtained at an  $o/f$  of 2.4 with the impinging-sheets injector. This efficiency is comparable with that obtained with the impinging-jet injector. Gas velocity, however, showed impinging sheets to be less effective than impinging jets. Velocity increased rapidly near the injector but the rate decreased downstream, indicating that mixing with impinging sheets was not as effective as with impinging jets. Further evidence, obtained from patterns burned in the plastic chambers, indicates that oxygen sheets were cutting through the plane of impingement. Variations in impingement angle and method of forming sheets might improve this condition. Repetitive arrangements of pattern would also be expected to improve mixing.

It was concluded that direct mixing of fuel and oxidant by the injection process definitely shortens the time necessary to reach a given stage of combustion. Mixing after atomization appeared to be about as effective as mixing before atomization.

#### Summary of Atomization and Mixing

A comparison of injector performance showed that atomizing the oxygen and fuel increased the  $c^*$  efficiency by 11 and 31 percentage points, respectively. Mixing by the impinging-jet injector produced an additional increase of 8 percentage points. The contribution to  $c^*$  may be divided among these and other factors as follows:



The values shown are only meant to illustrate the relative importance of atomization and mixing. The absolute magnitude may vary with chamber and injector design. For example, a comparison based on a shorter chamber length would increase the contribution of mixing.

Mixture distribution. - The spatial variations in mixture ratio also affect combustion efficiency. This mixture distribution is qualitatively indicated by the shape of the curves of  $c^*$  against  $o/f$  shown in table II. If the curve is relatively flat, burning is probably occurring at mixture ratios quite different from the set  $o/f$ . The resulting dissimilar products probably leave the rocket before mixing thoroughly or reaching equilibrium. This condition indicates poor initial mixture distribution and must be charged partly to the injector. Peak theoretical performance would be difficult to obtain in such a case.

On the other hand, if the curve of  $c^*$  against  $o/f$  follows the shape of the theoretical curve, good mixing is indicated. Most of the burning must occur close to the set  $o/f$  or chamber mixing must be efficient enough to allow an equilibrium to be reached before the gases leave the chamber. Thus, mixing with respect to mixture distribution becomes important in obtaining high efficiency.

Flow patterns. - A general tendency for flow of burning and burned gases to issue from between the fuel-oxidant interface was observed. This is shown, for example, in the gas-flow patterns for the parallel-sheets injector (fig. 7(c)). Flow out of the interface tended to separate the fuel from the oxidant. A certain amount of large-scale turbulence was generated near the injector as a result of this flow, but the mixing effectiveness of this turbulence did not appear large. This condition was evident for all injectors other than the impinging-jet and fuel-cone injectors.

Nonluminous zones were evident in many of the combustion photographs. These zones generally persisted throughout the length of the chamber. The photographs in figure 7(c) illustrate this condition. The photographs imply that mass diffusion due to turbulence is not large. Once established, a region or pocket of poor preparation or burning is not readily mixed with other gases.

More detailed differences between the flow patterns and combustion photographs may be seen in figures 2 to 11.

Gas velocities. - The agreement between experimental  $c^*$  and measured velocities was reasonably good for all test conditions. The deviation between the final and calculated velocity was generally less than 5 percent. A velocity calculated from the experimental  $c^*$  is shown in the curves of figures 2 to 11. In view of the difficulty in measuring a velocity at the nozzle entrance, the deviations appear to be within measurement accuracy.

Performance was measured with short chambers in some cases. This was done to determine whether or not completeness of combustion could be predicted from the gas velocity. Chambers 2 and 4 inches long were used with the parallel-sheets injector. The results are shown in figure 7(b). The efficiency of  $c^*$  at an  $o/f$  of 2.4 was 76 percent with the 4-inch chamber and 68 percent with the 2-inch chamber. These results agree qualitatively with those predicted from the velocity profile in the 8-inch chamber. Quantitative agreement, however, is lacking. This may be caused by a change in the combustion process in short chambers. However, final velocities agree with  $c^*$ , and the gas velocity serves as a qualitative picture of completeness of combustion.

Chambers 4 and 2 inches long were also run with the long-stream-length impinging-jet injector. The performance is shown in figure 9(b). In the low  $o/f$  region, the two chambers exhibited identical performance, which was about 8 percent lower than that with the 8-inch chamber. The result is again in qualitative agreement with the performance predicted from gas-velocity measurements in the 8-inch chamber.

Performance with plastic chambers. - The  $c^*$  with plastic chambers was higher than with steel chambers for most injectors with efficiencies less than 80 percent. Burning of plastic and the low heat transfer through the walls are believed responsible for this effect. Except for the low-efficiency injectors, the agreement between plastic and steel chambers was good. The observations made in plastic chambers are assumed to be typical of normal injector characteristics.

Instabilities. - Screaming operation was often encountered during this investigation. It was usually characterized by severe flow oscillation in the chamber at a frequency of about 3000 cycles per second.

High-frequency sound oscillations were also evident. The  $c^*$  always increased during such operation.

Streak photographs and 3000-frame-per-second photographs of screaming operation are shown for two injectors in figure 16. The saw-tooth luminous traces in the streak photographs occur because longitudinal waves traveled back and forth at a rate of about 3000 cycles per second. The nonluminous pockets shown in the motion pictures occurred at the same frequency.

The efficiency of  $c^*$  during screaming was above 80 percent for all injectors. Injectors that performed well during stable operation also performed best during screaming operation. Figure 17 shows  $c^*$  for several injectors. Highest efficiency, 93.5 percent at an  $o/f$  of 2.4, was obtained with the long-stream-length impinging-jet injector. These data are uncorrected for heat transfer. Limited heat-transfer data were obtained for the impinging-jet injector; the rate was greater than 4 Btu per second per square inch. Corrected for heat transfer, the  $c^*$  would lie close to the theoretical equilibrium curve.

Instability characteristics of the various injectors are summarized in table II. The impinging-jet injectors were always unstable at an  $o/f$  greater than about 2.0. With the fuel-atomizing injectors, instability again was prevalent but at a lesser intensity. The parallel and impinging-sheets injectors exhibited both combustion stability and relatively high performance. The other injectors were basically stable except that the wide-space parallel-jet injector exhibited an occasional performance jump. This jump was not accompanied by an audible scream.

These stability characteristics may be related to the injection process. Combustion was quite stable when both propellants were atomized before they were mixed; such preparation occurred, in part, for both the parallel and impinging-sheets injectors. These injectors, in effect, produced a mixture of drops in the chamber. It is reasonable to expect that such a mixture is not readily disturbed by a pressure wave.

The preparation process of the other injectors may be more sensitive to a disturbance. Impinging-jet injectors are sensitive to misalignment of jets, and a pressure wave may induce such a misalignment. For the fuel-atomizing injectors, a pressure wave may also disturb fuel impingement, or the wave may periodically improve mixing by inducing extreme turbulence. These mechanisms could be the coupling between reaction and a pressure wave that is necessary for the perpetuation of instability.

The results here are not conclusive, and more study is required to determine the effect of preparation on instability. At present, it appears that proper injection can minimize combustion instability by making the prepared propellants insensitive to chamber disturbances.

The tendency to scream did not appear related to the heat-release rate in the chamber. By using chamber velocity as a criterion, it can be seen that instability was prevalent with both uniform and concentrated heat releases. The intensity of screaming was higher, however, for the impinging-jet injectors, which completed a large percentage of the reaction close to the injector.

Starting. - The starting characteristics of the injectors are summarized in table II. These characteristics were obtained from the analysis of streak photographs. Some typical photographs of starting are presented in the detailed performance (figs. 2 to 11).

The engine starts also appear to correlate with injection processes, as did combustion instability. Intermittent detonations at the start with longitudinal and lateral oscillations during the transition period were characteristic of the impinging-jet injectors. This condition diminished somewhat for the fuel-atomizing injectors. It was entirely absent for the parallel and impinging-sheets injectors. Therefore, smooth starts and stable operation and, conversely, turbulent starts and screaming tendencies appear to be closely related.

#### SUMMARY OF RESULTS

An investigation of injection methods in a 200-pound-thrust rocket engine has indicated the following results for liquid oxygen and heptane propellants:

Comparison of injector performance during stable operation showed that the injector must atomize and mix both propellants for high-efficiency combustion. Atomizing the heptane, however, is much more important than atomizing the oxygen. In a constant-characteristic-length chamber, heptane atomization increased the characteristic exhaust-velocity efficiency by about 31 percent compared with 11 percent for oxygen atomization. Mixing the propellants reduced the time required to complete combustion. Mixing before or after atomization appeared to be equally effective; however, premixing the propellants resulted in destructive explosions.

Screaming operation was often encountered. The occurrence of screaming was related to the injection method. Impinging-jet and fuel-atomizing injectors were very unstable. Parallel and impinging-sheets arrangements, however, generally performed stably. Engine starts for these injectors showed similar characteristics. This result indicates a possible relation between combustion stability and the sensitivity of the injection method to a chamber disturbance.

## CONCLUDING REMARKS

The results obtained have indicated desirable properties of an injector element for the liquid oxygen - heptane propellant combination. The best combination of performance characteristics should be obtained by an injection method in which (1) heptane atomization is emphasized, and (2) a characteristic of mixing after atomization is predominant. The performance with such injection may be expected to include (1) high-efficiency combustion in a minimum volume, (2) stable combustion, and (3) smooth engine starts. These observations, however, must be treated with reservation. The tests were made with a single injector element in a low-thrust engine. Extension of the data to large thrust and repetitive pattern injectors must be confirmed.

Lewis Flight Propulsion Laboratory  
National Advisory Committee for Aeronautics  
Cleveland, Ohio, March 24, 1955

## APPENDIX A

## SYMBOLS

The following symbols are used in this report:

A	area, sq ft
$c^*$	characteristic exhaust velocity, ft/sec
g	gravitational constant, 32.2 ft/sec <sup>2</sup>
$L^*$	characteristic chamber length, in.
M	Mach number
m	molecular weight, (lb)(mole)
o/f	oxidant-fuel weight ratio
P	stagnation or total pressure, lb/sq ft abs
p	static pressure, lb/sq ft abs
q	dynamic pressure, lb/sq ft abs
R	universal gas constant, (ft)(lb)/(lb)(mole)(°R)
T	total temperature, °R
t	static temperature, °R
V	gas velocity, ft/sec
w	propellant flow rate, lb/sec
$\gamma$	ratio of specific heats
$\rho$	density of combustion gases, lb/cu ft

## Subscripts:

c	combustion chamber
t	nozzle throat

## APPENDIX B

## DERIVATION OF CHARACTERISTIC EXHAUST VELOCITY

The derivation of the equation for the determination of the characteristic exhaust velocity in terms of the chamber gas velocity is as follows:

The dynamic pressure within the chamber is given by

$$q_c = \frac{1}{2} \frac{\rho_c V_c^2}{g} \quad (B1)$$

For a compressible gas at Mach numbers below 2,

$$\frac{P_c - P_c}{q_c} = 1 + \frac{1}{4} M_c^2 + \frac{2 - \gamma}{24} M_c^4 + \dots \quad (B2)$$

Chamber velocities seldom exceeded 300 feet per second in this investigation, resulting in Mach numbers of approximately 0.1. For these conditions, from equation (B2),  $(P_c - P_c)/q_c = 1$  within an error of approximately 0.25 percent. Therefore, from equation (B1) and the continuity equation,

$$P_c = P_c - \frac{1}{2} \frac{w_c V_c}{A_c g} \quad (B3)$$

From the perfect-gas law, equation (B3), and the continuity equation,

$$\frac{t_c}{m_c} = \frac{P_c}{\rho_c R} = \left( P_c - \frac{1}{2} \frac{w_c V_c}{A_c g} \right) \frac{A_c V_c}{w_c R} = \frac{P_c A_c V_c}{w_c R} - \frac{V_c^2}{2Rg} \quad (B4)$$

From the fundamental equation for characteristic velocity  $c^*$ ,

$$c^* = \frac{\sqrt{\gamma R g \frac{T_c}{m_c}}}{\gamma \left( \frac{2}{\gamma + 1} \right)^{\frac{\gamma + 1}{2(\gamma - 1)}}} \quad (B5)$$

From isentropic flow relations,

$$\frac{T_c}{t_c} = 1 + \frac{\gamma - 1}{2} M_c^2$$

For  $M_c \approx 0.1$  and  $\gamma \approx 1.2$ ,  $T_c/t_c \approx 1.001$  or  $T_c = t_c$  within an error of approximately 0.1 percent. Substituting in equation (B5),

$$\frac{t_c}{m_c} = \gamma \left( \frac{2}{\gamma + 1} \right)^{\frac{\gamma+1}{\gamma-1}} \frac{(c^*)^2}{Rg} \quad (B6)$$

Equating equations (B4) and (B6) and simplifying, using

$$c^* = \frac{P_c A_t g}{w}$$

gives

$$\gamma \left( \frac{2}{\gamma + 1} \right)^{\frac{\gamma+1}{\gamma-1}} (c^*)^2 = \frac{c^* A_c V_c}{A_t} - \frac{V_c^2}{2} \quad (B7)$$

#### REFERENCES

1. Rupe, Jack H.: The Liquid-Phase Mixing of a Pair of Impinging Streams. Prog. Rep. No. 20-195, Jet Prop. Lab., C.I.T., Aug. 6, 1953. (ORDCIT Proj. Contract DA-04-495, Ord 18, Dept. Army Ord. Corps.)
2. Northup, R. P.: An Experimental Investigation of the Flow and Stability of Liquid Streams from Small Orifices Discharging into a Gaseous Atmosphere. Rep. R51A0512, Spec. Proj. Eng. Div., Apparatus Dept., General Electric Co., Feb. 1951. (Proj. Hermes (TUL-2000A.))
3. Szlachain, J. A.: Notes on Atomization of a Liquid at Low Injection Pressures. Meteor Rep. BAC-5, Proj. Meteor, Bell Aircraft Corp., June 20, 1947. (Contract NOrd 9876.)
4. Heidmann, Marcus F., and Humphrey, Jack C.: Fluctuations in a Spray Formed by Two Impinging Jets. NACA TN 2349, 1951.

5. Weisenberg, I. J., and Novotny, R. J.: Experimental and Theoretical Investigations of Rocket Engines to Determine Operating Characteristics of Various Design Parameters. Rep. R.M.I. 294-DH, Design Handbook, Reaction Motors, Inc., June 24, 1952. (Contract NOa(s) 9502.)
6. Datner, P. P., and Dawson, E. E.: Testing of Repetitive-Pattern Injectors in 1000-Lb Thrust Chambers with Chamber-to-Throat Area Ratios of 4.5 Using WFNA and JP-3. Rep. 555, Aerojet Eng. Corp., July 25, 1952. (Contract AF 33(038)-2733, Proj. MX-1079, E.O. No. 539-44.)
7. Baker, Dwight I.: Mixture Ratio and Temperature Surveys of Ammonia-Oxygen, Rocket-Motor Combustion Chambers. Rep. No. 25-2, Jet Prop. Lab., C.I.T., Jan. 29, 1954. (Dept. Navy, Bur. Aero. Contract NOa(s)-53729.)
8. Bellman, Donald R., Humphrey, Jack C., and Male, Theodore: Photographic Investigation of Combustion in a Two-Dimensional Transparent Rocket Engine. NACA Rep. 1134, 1953. (Supersedes NACA RM E8F01.)
9. Olsen, M. N.: Photographic Studies of Injectors. Vol. III. Rep. RMI-294-F, Reaction Motors, Inc., Nov. 5, 1952. (Contract NOa(s) 9502.)
10. Trent, C. H.: A Study of Combustion of WFNA and JP-3 in Rocket Thrust Chambers. Rep. No. 628, Aerojet Eng. Corp., Nov. 15, 1952. (Contract AF33(038)-2733, Item 30, Proj. MX-1079.)
11. Berman, K., and Cheney, S. N.: Rocket Motor Instability Studies. Rep. No. R53A0518, Guided Missiles Dept., General Electric Co., Aug. 1953. (Contract DA-30-115-ORD-23, Proj. Hermes TUL-2000A.)
12. Male, Theodore, Kerslake, William R., and Tischler, Adelbert O.: Photographic Study of Rotary Screaming and Other Oscillations in a Rocket Engine. NACA RM E54A29, 1954.

TABLE I. - DESCRIPTION OF EXPERIMENTAL INJECTORS

Injection process	Injector	Figure	Remarks
No mixing or atomization	Parallel jets, wide space	2	Distance between jet surfaces, 0.14 and 0.0125 in., respectively
	Parallel jets, close space	3	
Atomization without mixing Atomization of oxidant	Parallel oxidant sheets, fuel jet	4	Oxidant atomized by deflector plates
Atomization of fuel	Parallel fuel sheet, oxidant jets	5	Fuel atomized by self-impingement and jet impingement on upturned end of rod, respectively
	Fuel cone, parallel oxidant jets	6	
Atomization of both propellants	Parallel sheets	7	Oxidant atomized by deflector plates, fuel by self-impingement
Mixing without atomization	Premix	8	Exit opening designed for pressure drop of 50 lb/sq in.
Mixing with atomization Mixing before atomization	Impinging jets, long stream length	9	Stream length before impingement, 1/4 and 1/8 in., respectively
	Impinging jets, surface impinging	10	
Mixing after atomization	Impinging sheets	11	Oxidant atomized by deflector plates, fuel by self-impingement

TABLE II. - SUMMARY OF EFFECTS OF PROPELLANT PREPARATION ON COMBUSTION AND PERFORMANCE

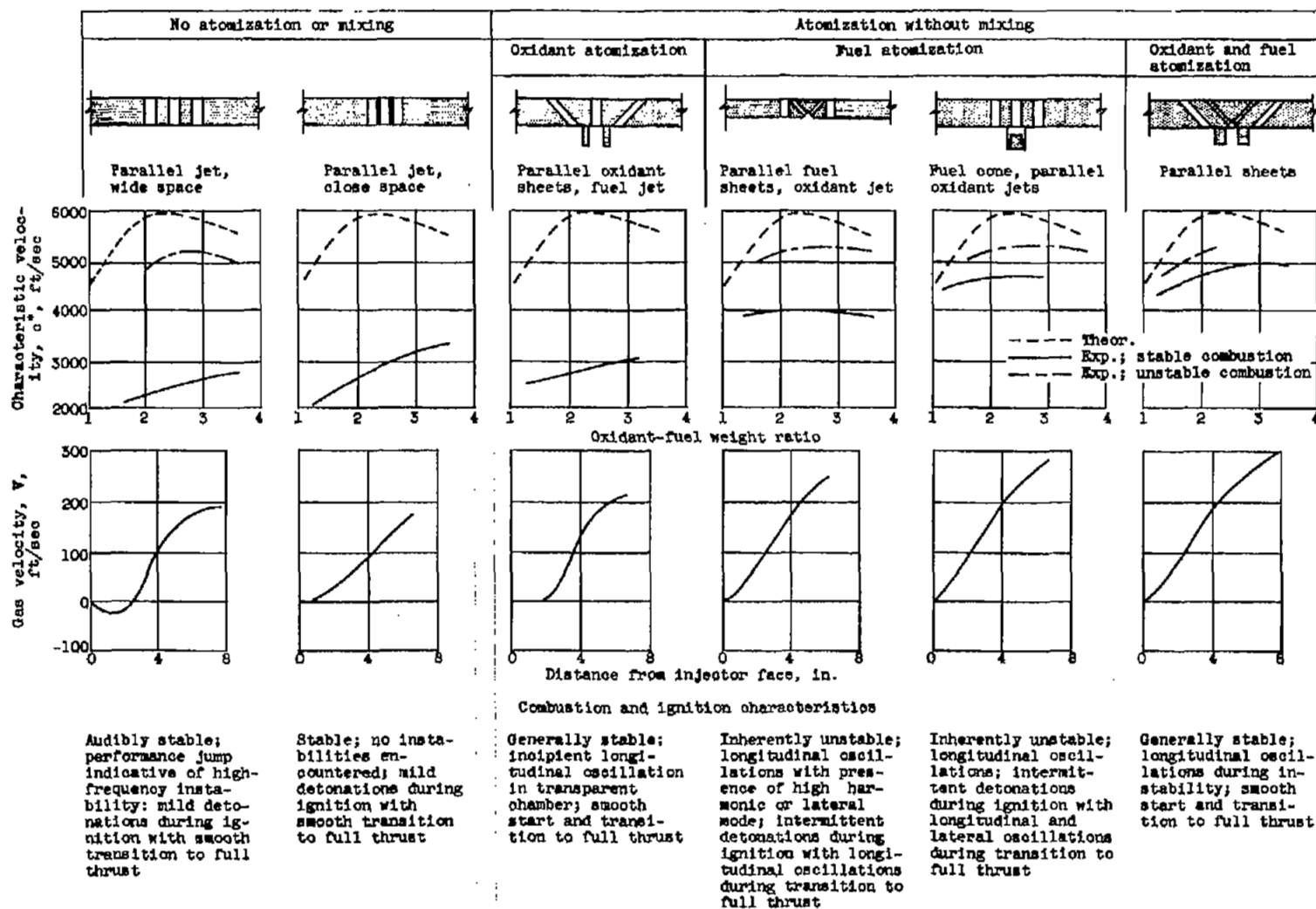
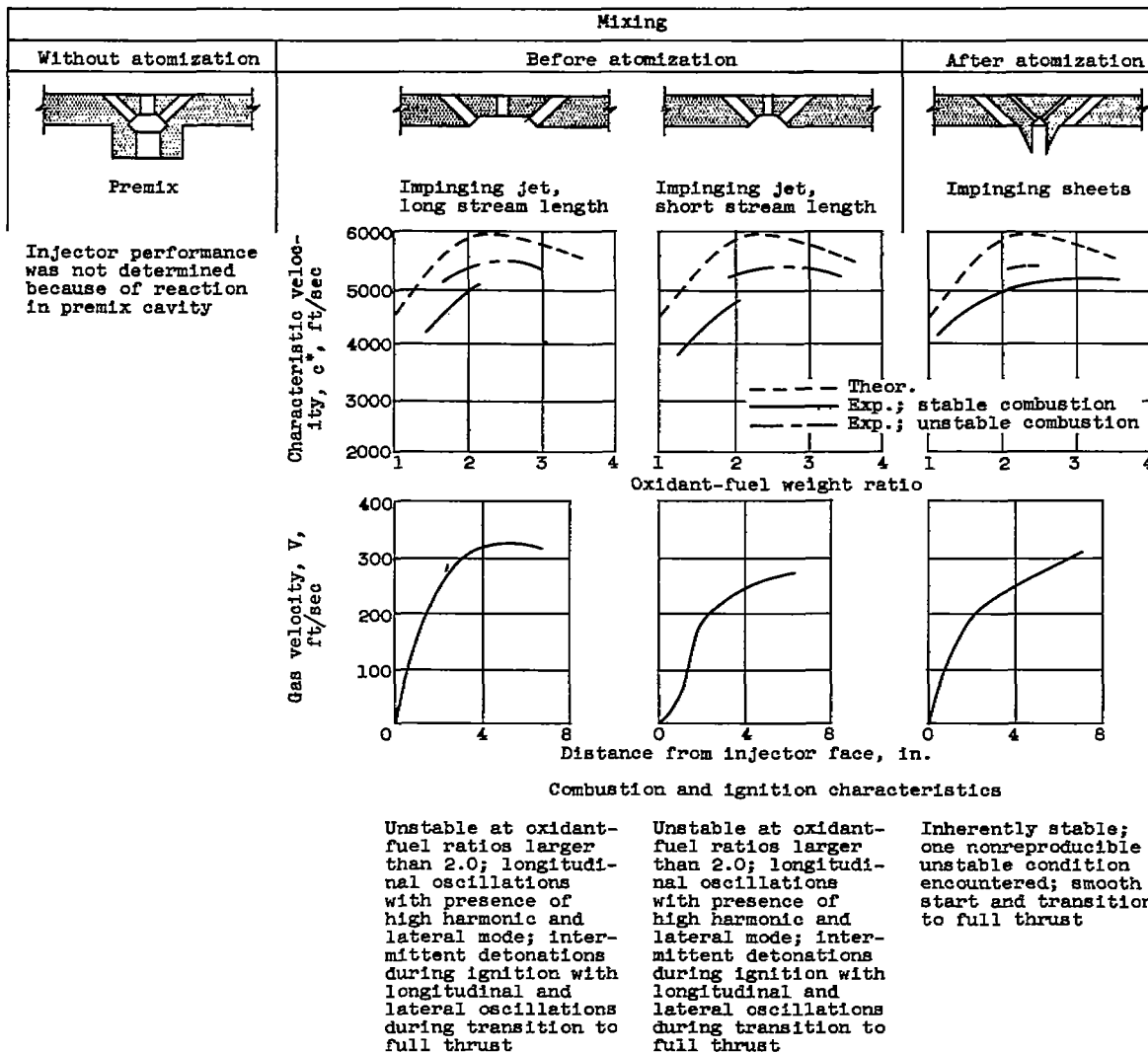
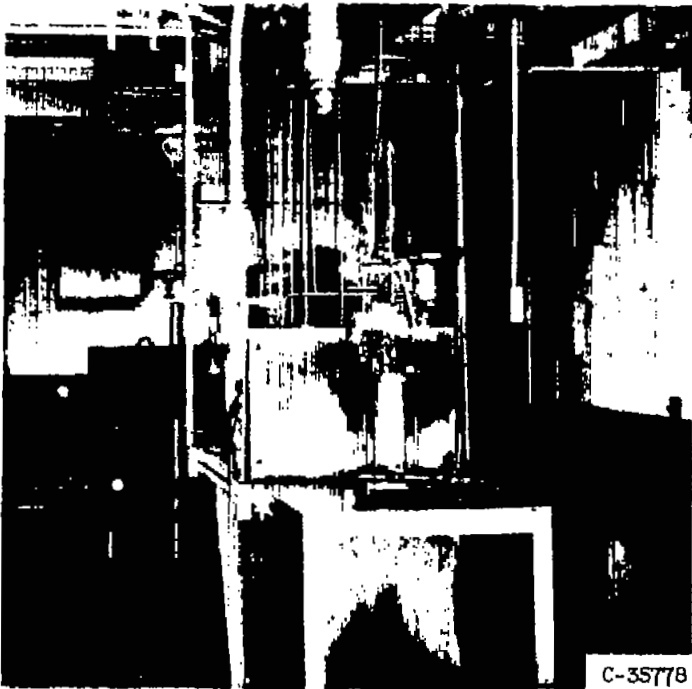


TABLE II. - Concluded. SUMMARY OF EFFECTS OF PROPELLANT PREPARATION ON COMBUSTION AND PERFORMANCE.



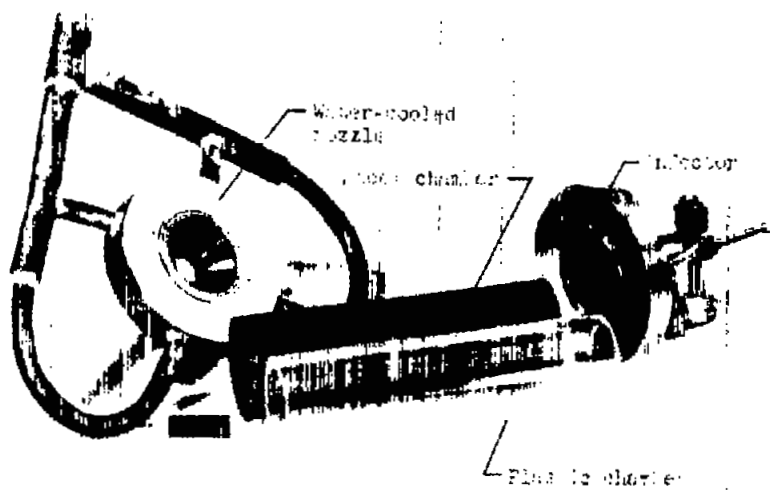
3572

UU-5 back



C-35778

(a) Rocket installation.

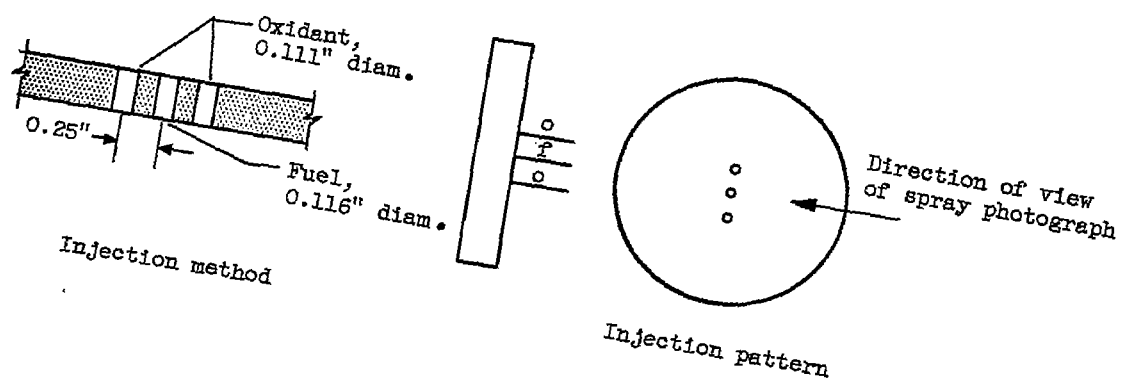


C-36874

(b) Engine components.

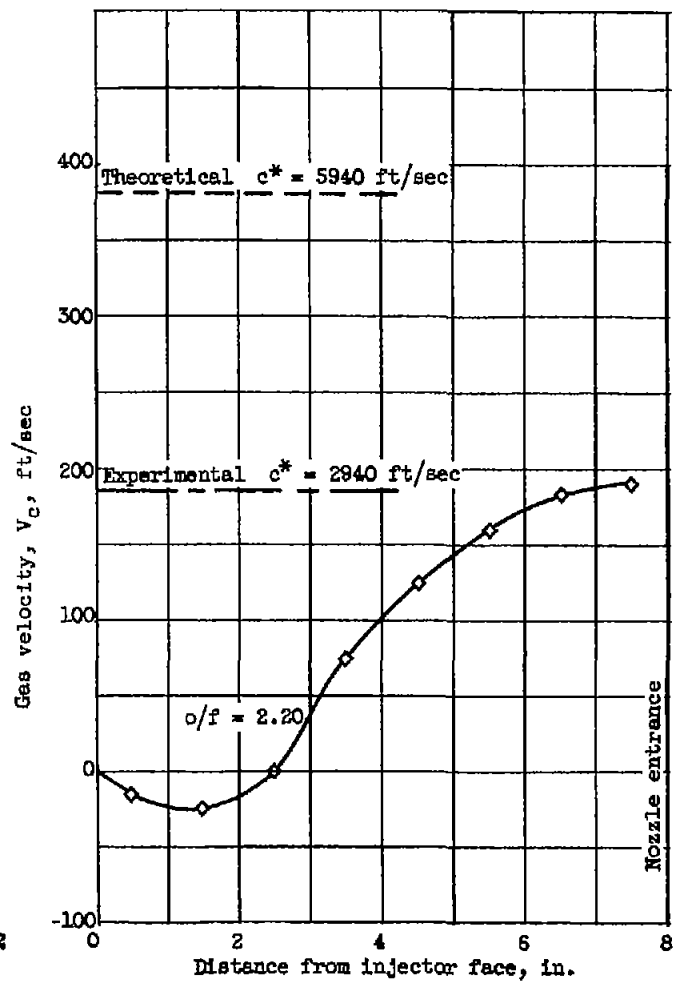
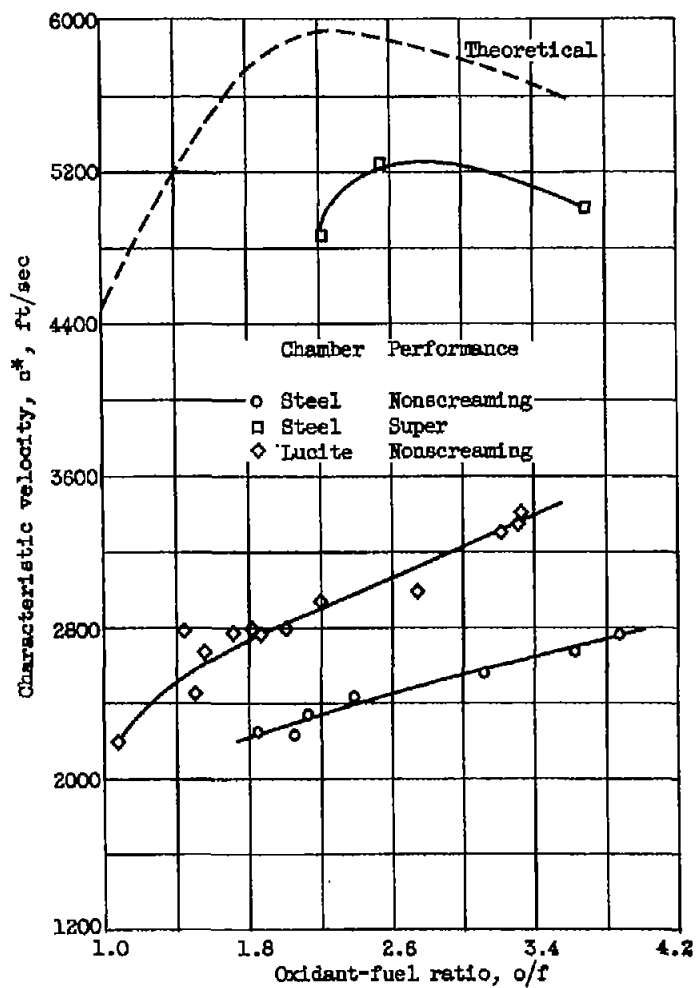
Figure 1. - Rocket installation and engine components.

3572



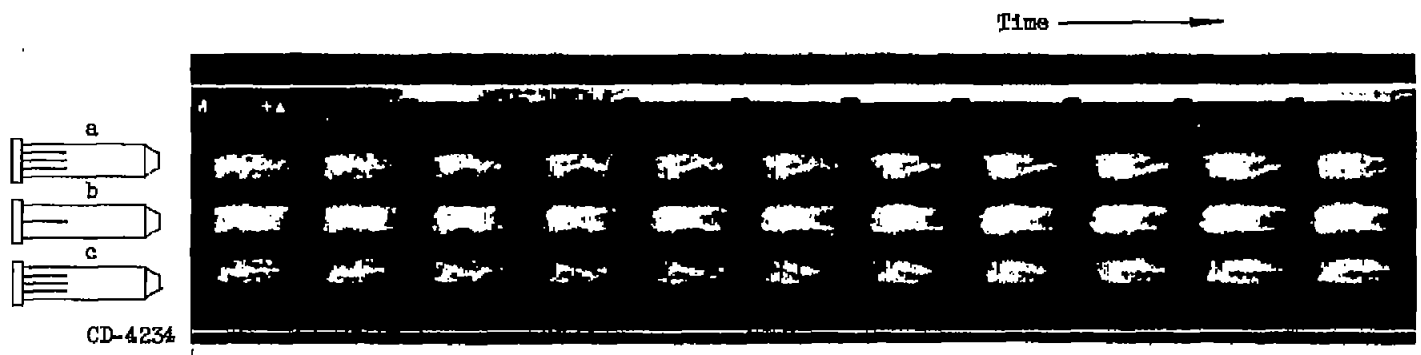
CD-4232

(a) Injector design and water-spray photograph.  
Figure 2. - Parallel-jets wide-space injector for no atomization or mixing.



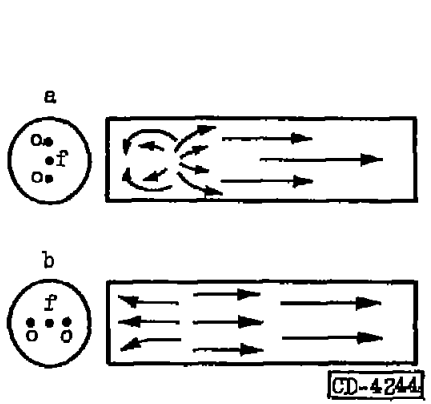
(b) Performance characteristics.

Figure 2. - Continued. Parallel-jets wide-space injector for no atomization or mixing.



CD-4234

Enlarged 3000-frame-per-second photographs of combustion



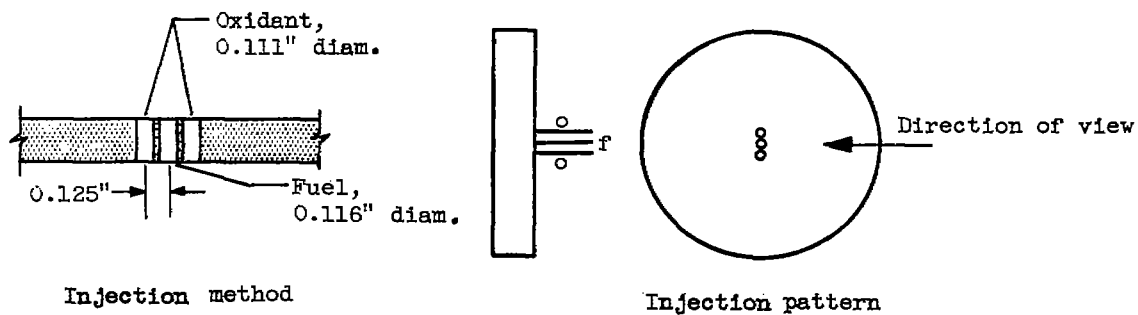
Gas-flow patterns observed from projected high-speed photographs



Streak photograph of ignition

(c) Combustion photographs and flow patterns.

Figure 2. - Concluded. Parallel-jets wide-space injector for no atomization or mixing.



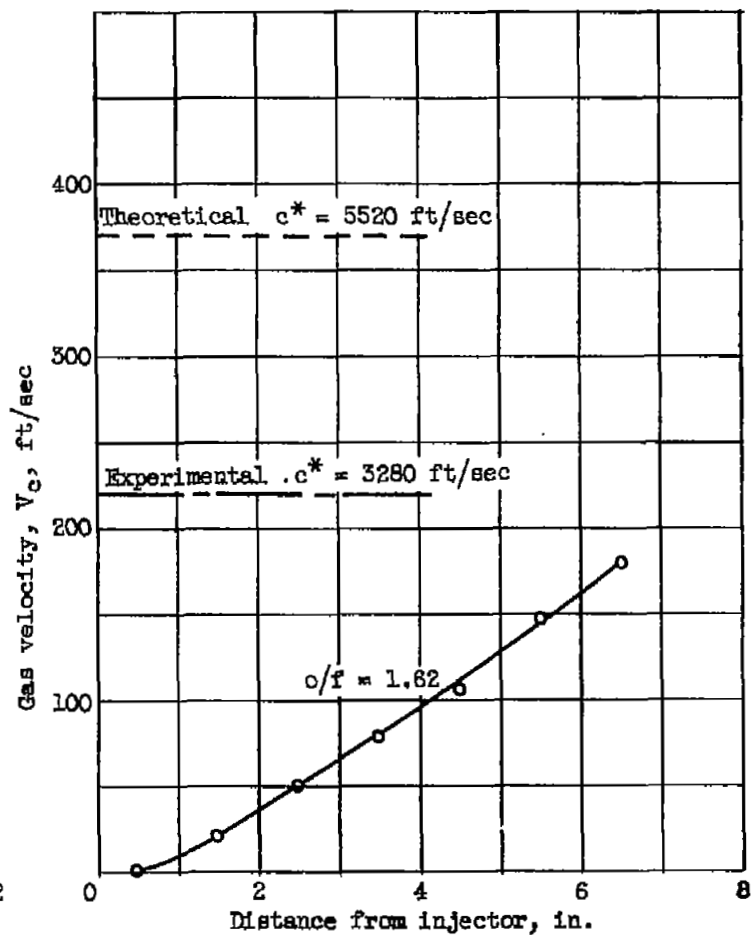
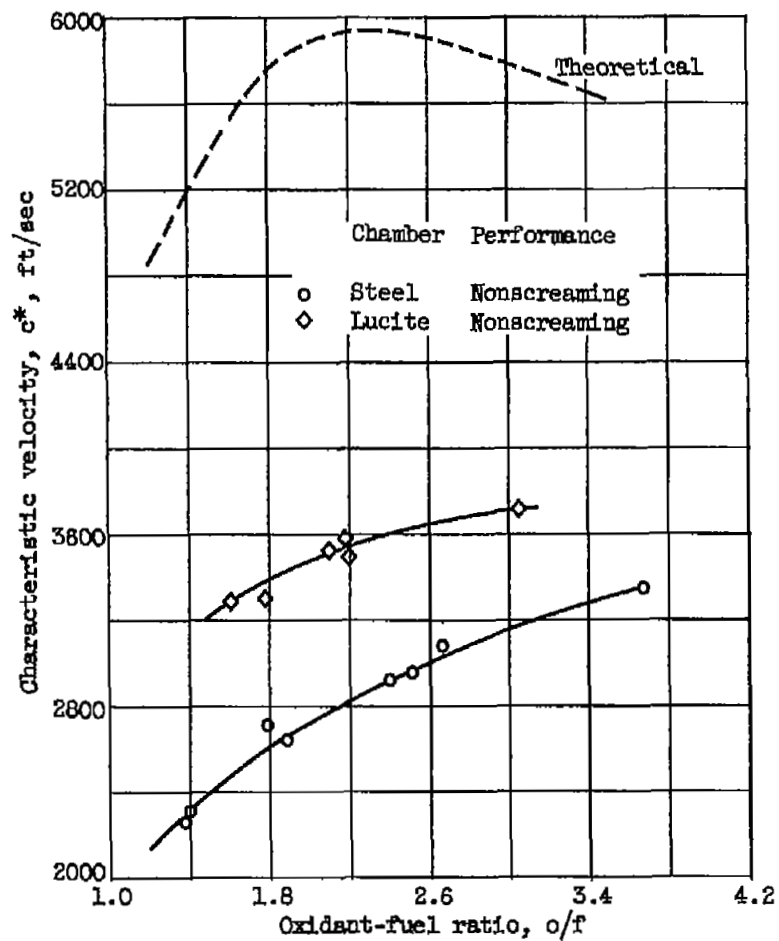
CD-4232



Spray photograph

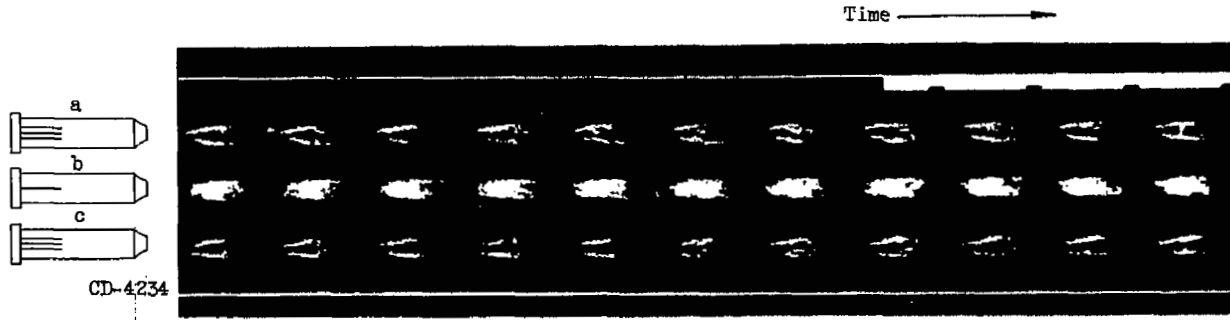
(a) Injector design and water-spray photograph.

Figure 3. - Parallel-jets close-space injector for no atomization or mixing.

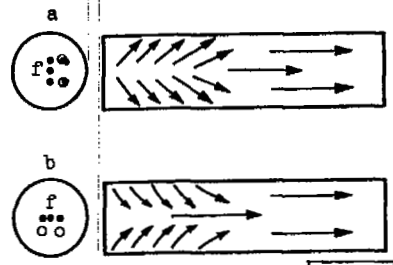


(b) Performance characteristics.

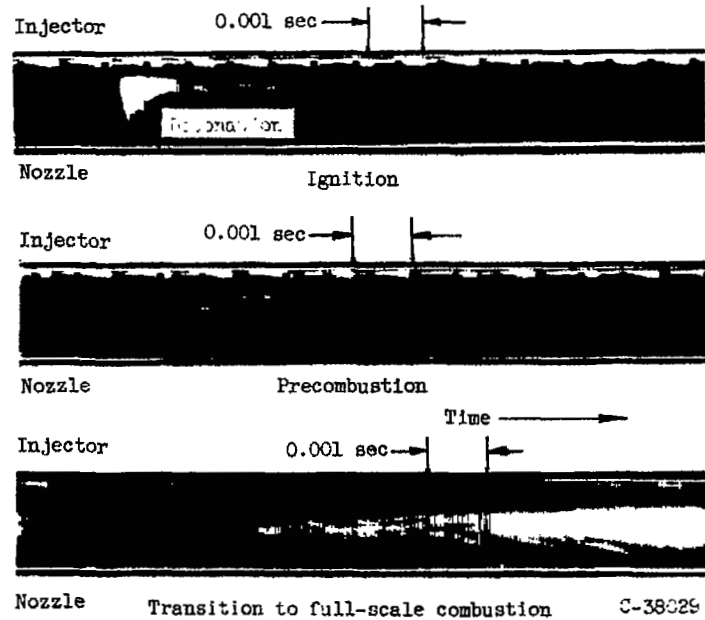
Figure 3. - Continued. Parallel-jets close-space injector for no atomization or mixing.



Enlarged 3000-frame-per-second photographs of combustion



Gas-flow patterns observed from projected high-speed photographs

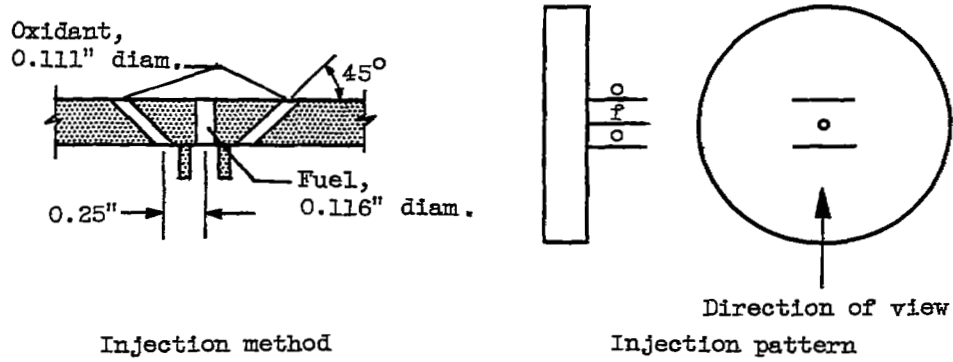


Streak photographs of ignition and starting

(c) Combustion photographs and flow patterns.

Figure 3. - Concluded. Parallel-jets close-space injector for no atomization or mixing.

3572



CD-4232

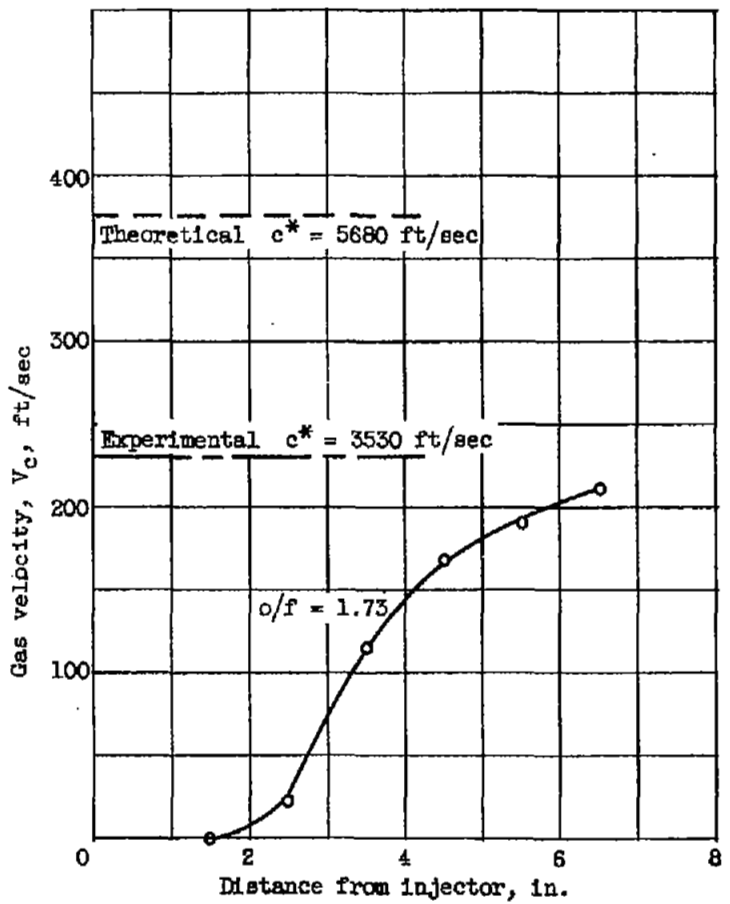
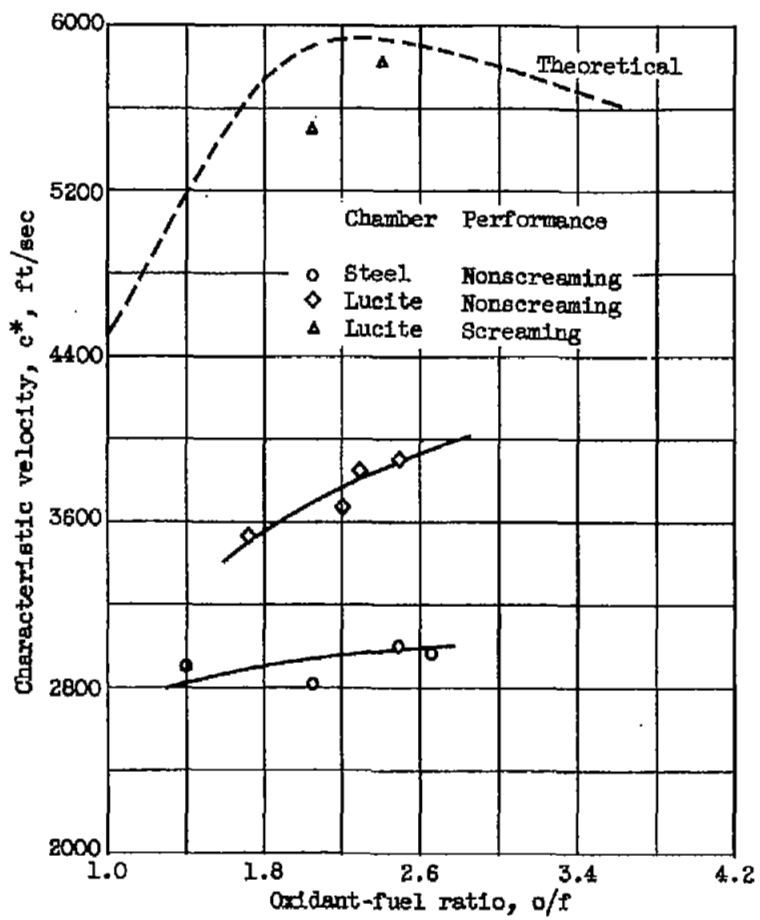
UU-4 BACK



Spray photograph

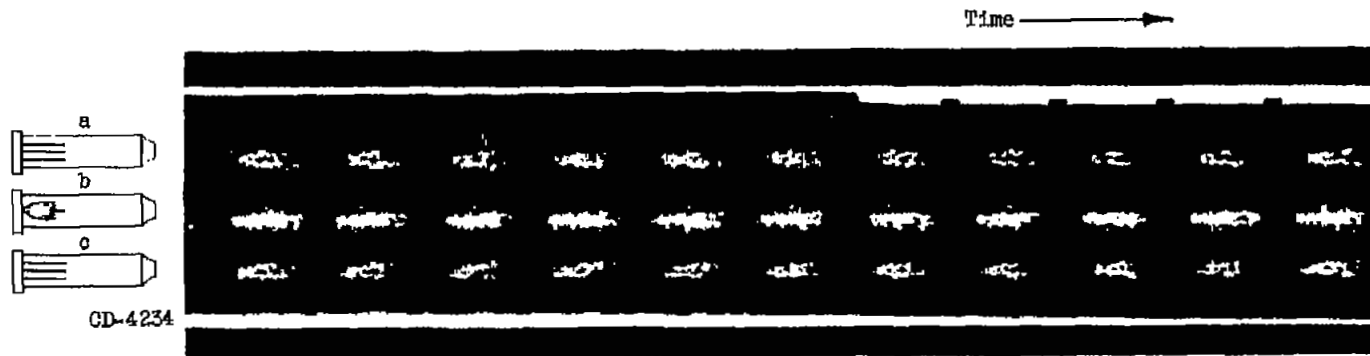
(a) Injector design and water-spray photograph.

Figure 4. - Parallel oxidant-sheets - fuel-jet injector for oxygen atomization

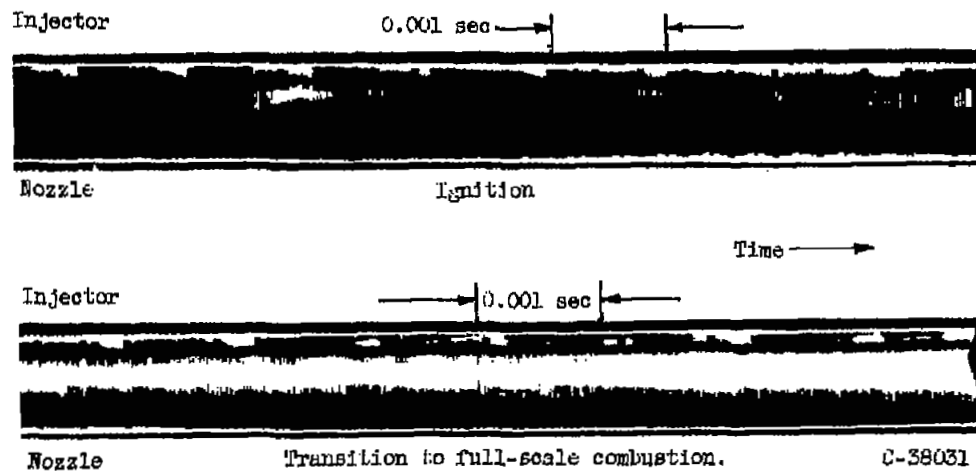


(b) Performance characteristics.

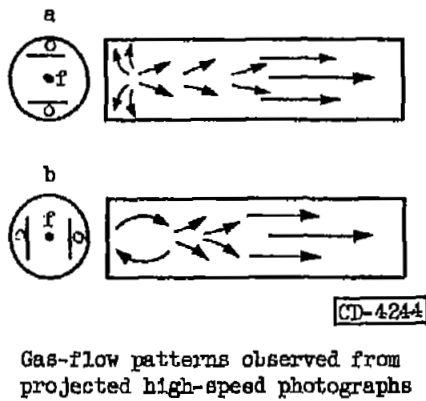
Figure 4. - Continued. Parallel oxidant-sheets - fuel-jet injector for oxygen atomization.



Enlarged 3000-frame-per-second photographs of combustion

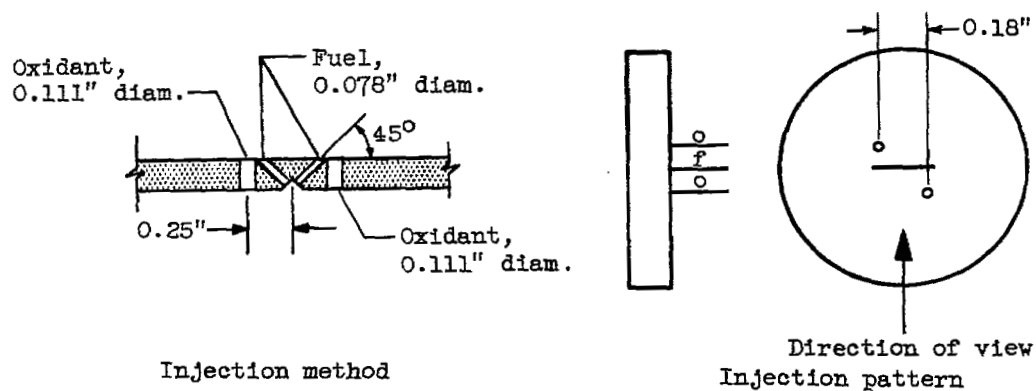


Streak photographs of ignition and starting



(c) Combustion photographs and flow patterns.

Figure 4. - Concluded. Parallel oxidant-sheets - fuel-jet injector for oxygen atomization.



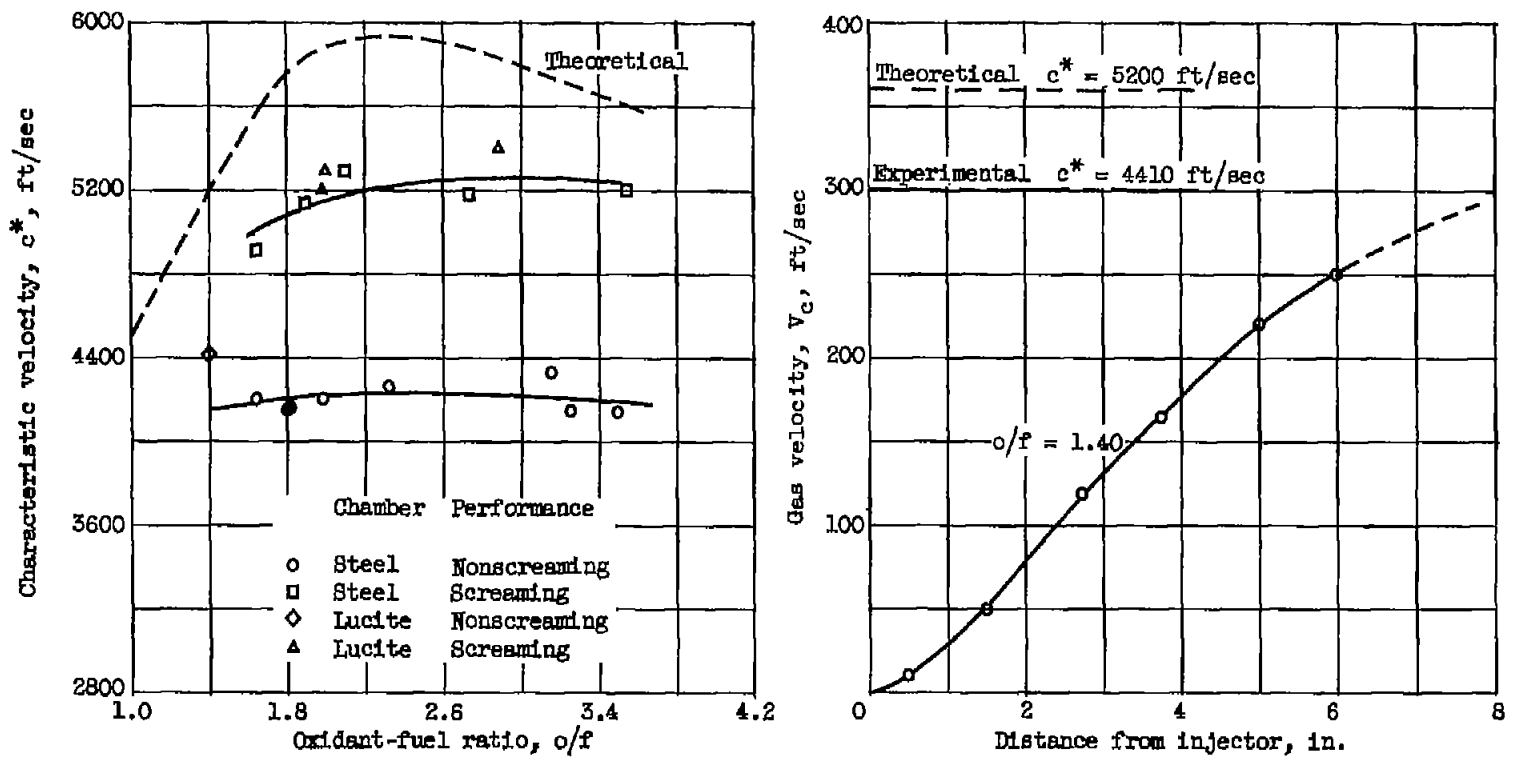
CD-4232



Spray photograph

(a) Injector design and water-spray photograph.

Figure 5. - Parallel fuel-sheet - oxidant-jets injector for fuel atomization.



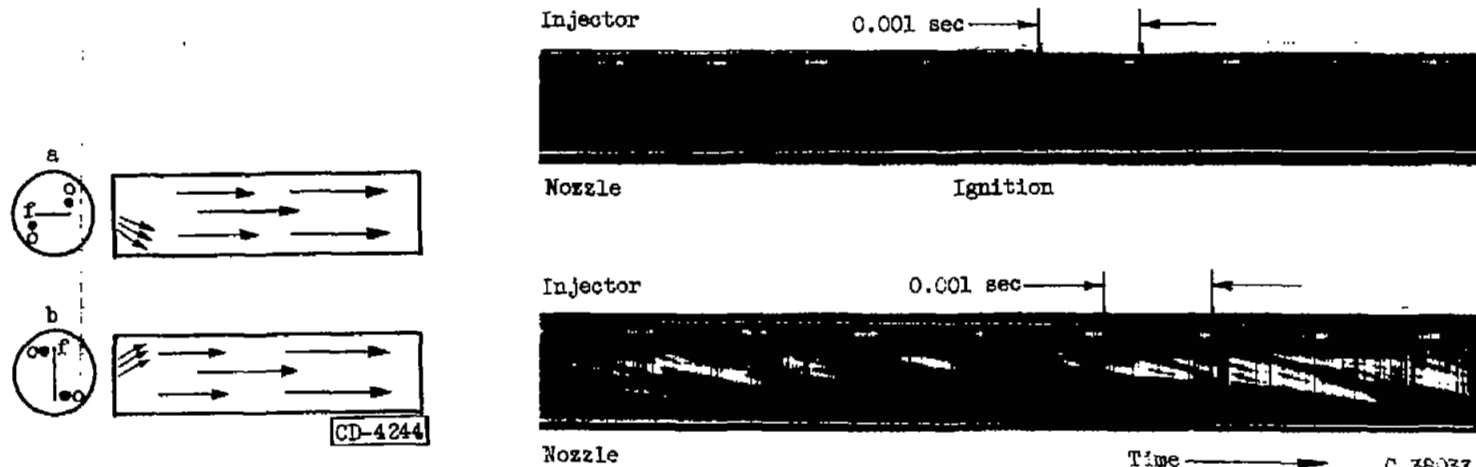
(b) Performance characteristics.

Figure 5. - Continued. Parallel fuel-sheet - oxidant-jets injector for fuel atomization.



Enlarged 3000-frame-per-second photographs of combustion

C-36033

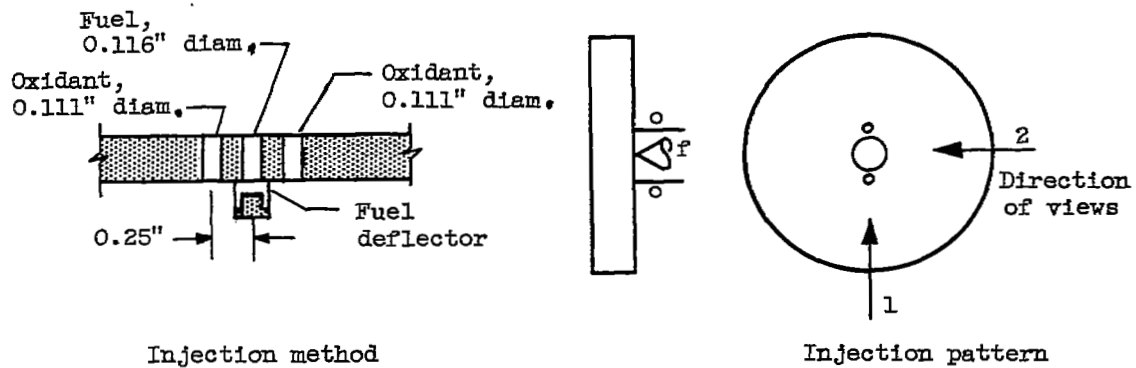


Gas-flow patterns observed from projected high-speed photographs

Streak photographs of ignition and starting

(c) Combustion photographs and flow patterns.

Figure 5. - Concluded. Parallel fuel-sheet - oxidant-jets injector for fuel atomization.



Injection method

Injection pattern

CD-4232



View 1

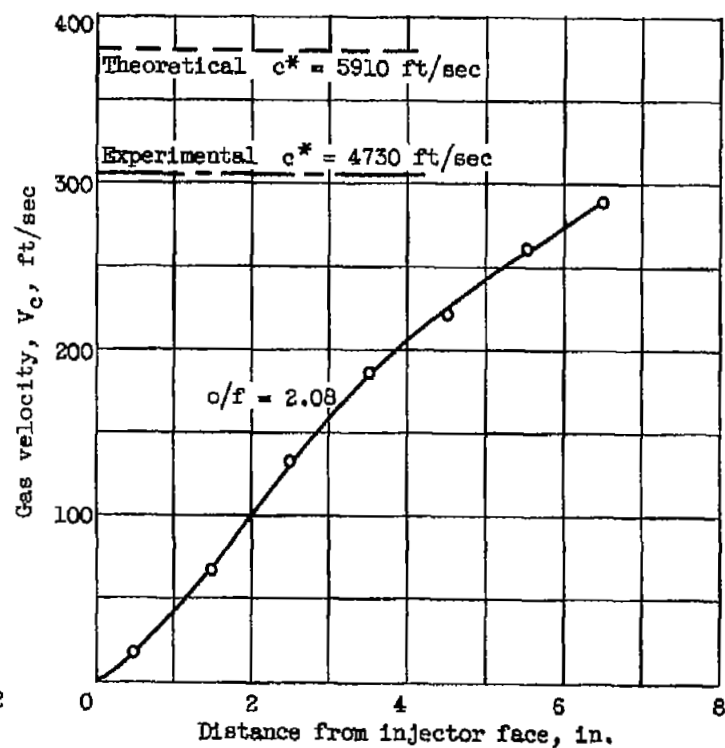
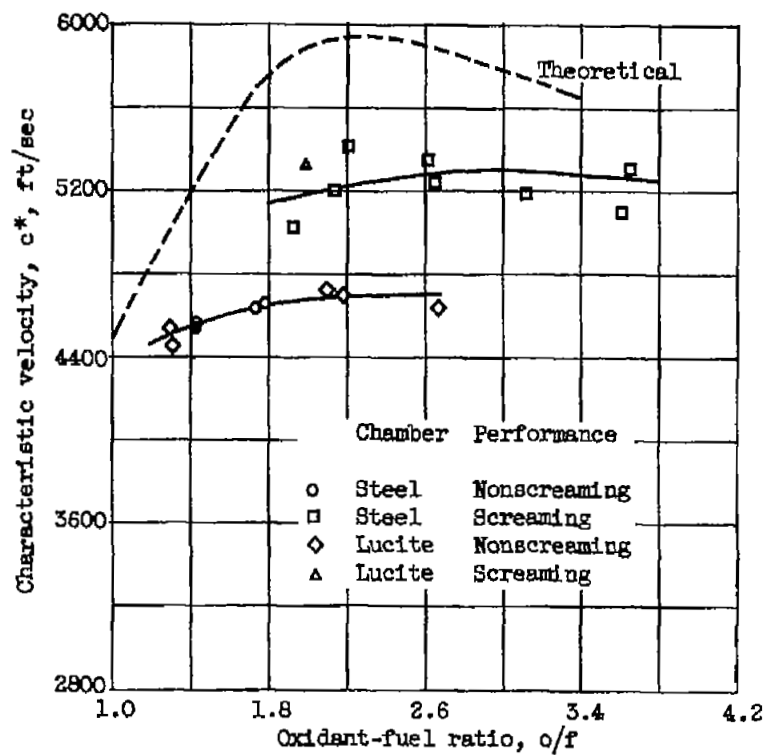


View 2

Spray photographs

(a) Injector design and water-spray photographs.

Figure 6. - Fuel-cone, parallel oxidant-jets injector for fuel atomization.

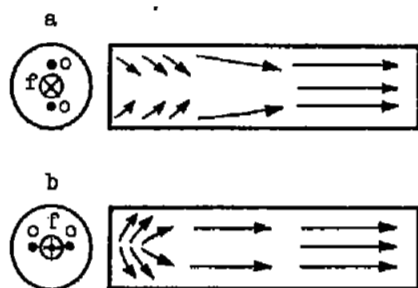
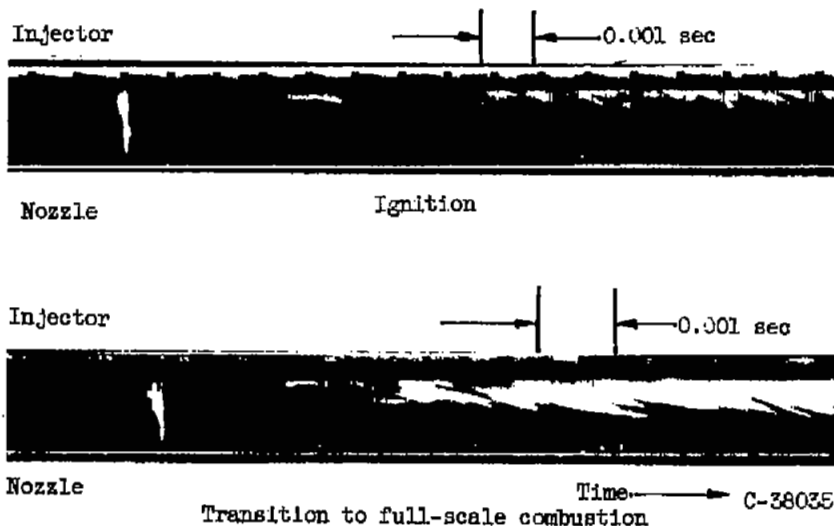


(b) Performance characteristics.

Figure 6. - Continued. Fuel-cone, parallel oxidant-jets injector for fuel atomization.



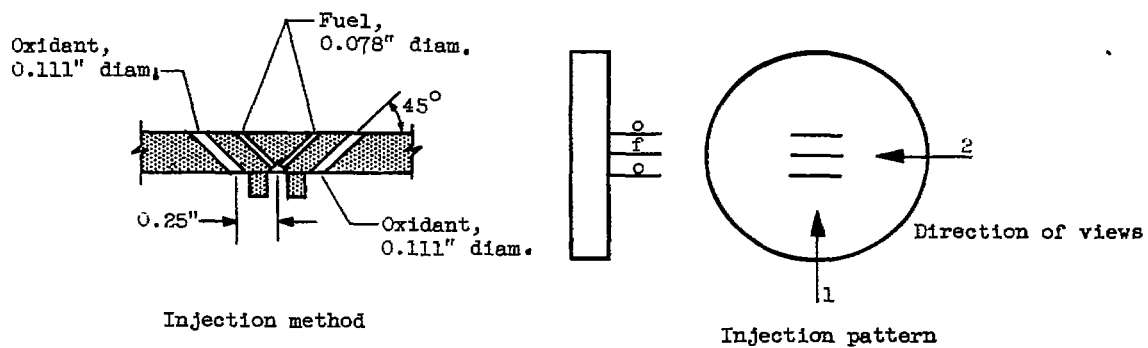
Enlarged 3000-frame-per-second photographs of combustion

Gas-flow patterns observed from  
projected high-speed photographs

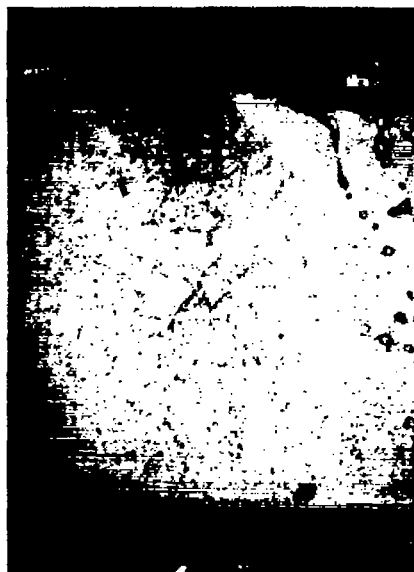
Streak photographs of ignition and starting

(c) Combustion photographs and flow patterns.

Figure 6. - Concluded. Fuel-cone, parallel oxidant-jets injector for fuel atomization.



CD-4232



View 1

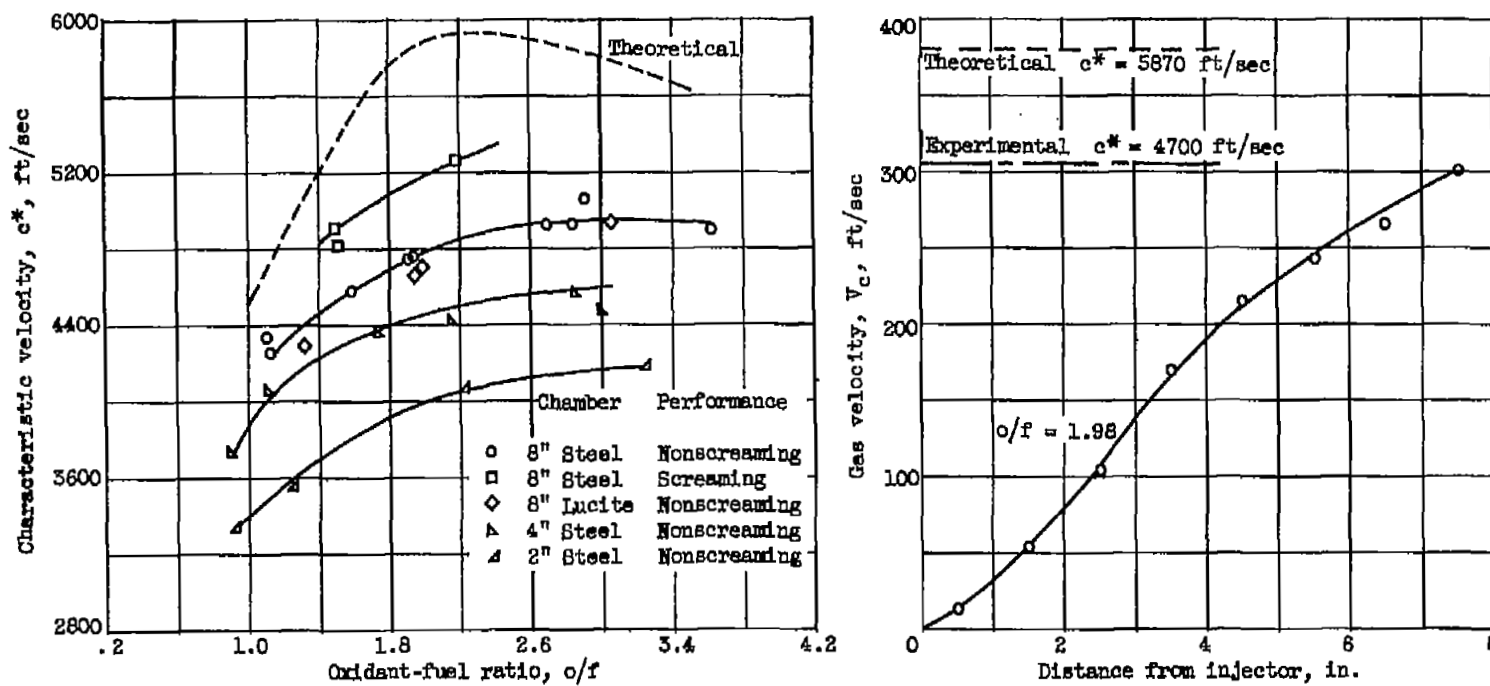


View 2

Spray photographs

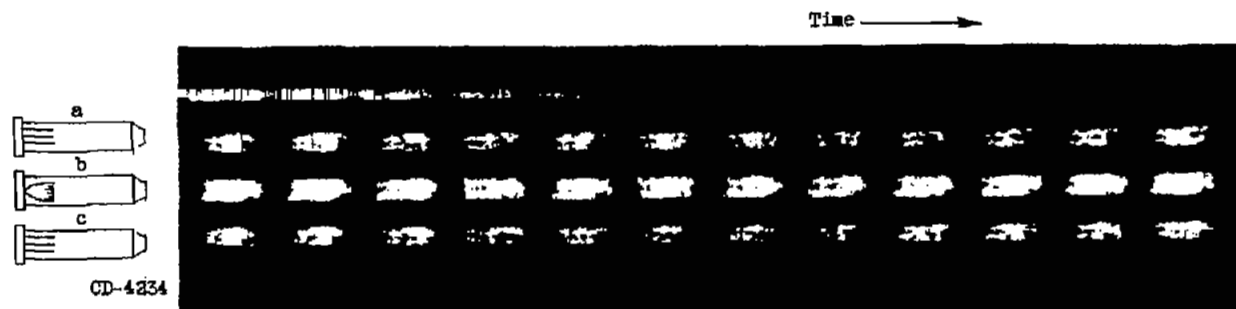
(a) Injector design and water-spray photographs.

Figure 7. - Parallel-sheets injector for atomization without mixing.

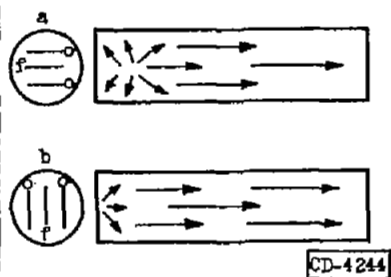


(b) Performance characteristics.

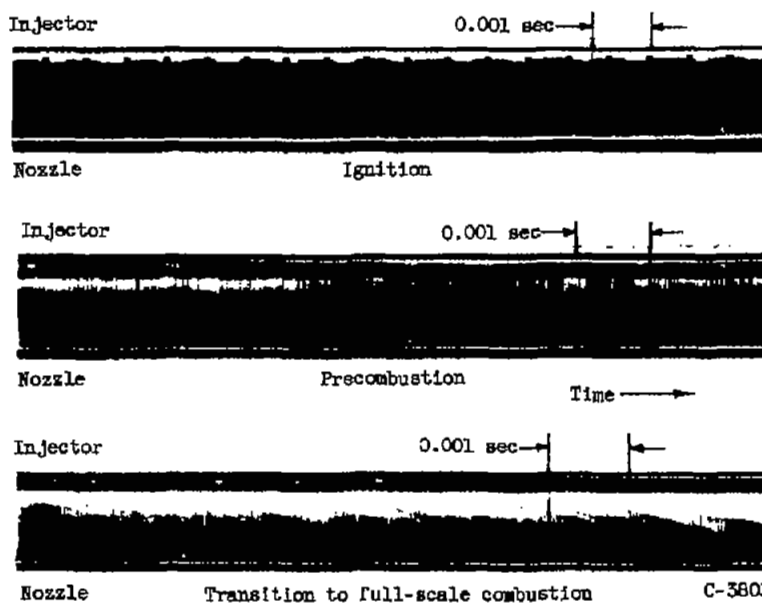
Figure 7. - Continued. Parallel-sheets injector for atomization without mixing.



Enlarged 3000- frame-per-second photographs of combustion



Gas-flow patterns observed from projected high-speed photographs

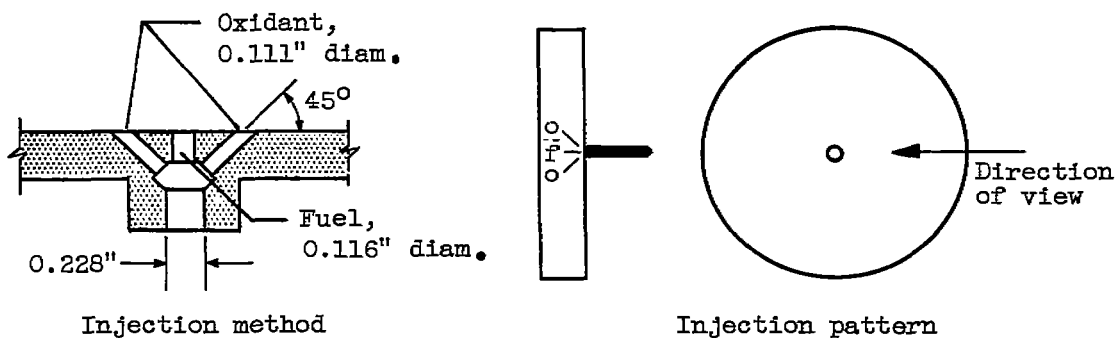


Streak photographs of ignition and starting

(c) Combustion photographs and flow patterns.

Figure 7. - Concluded. Parallel-sheets injector for atomization without mixing.

5572

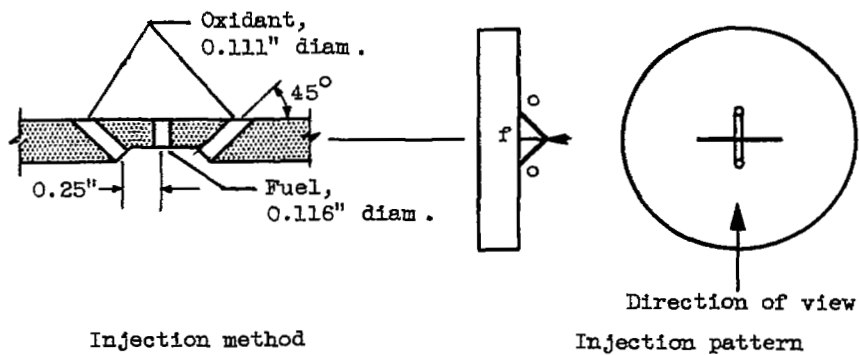


CD-4233



Spray photograph

Figure 8. - Premix injector design and water-spray photograph for mixing without atomization.

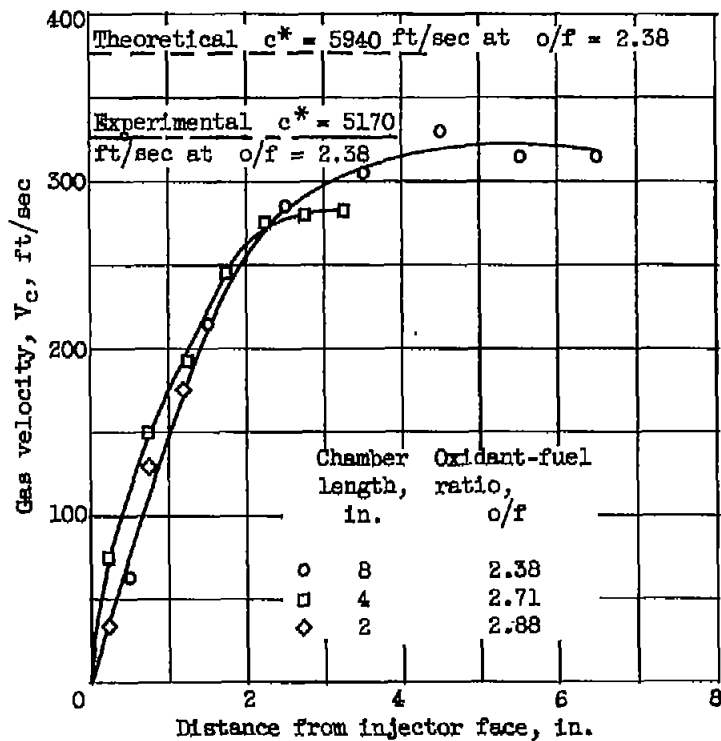
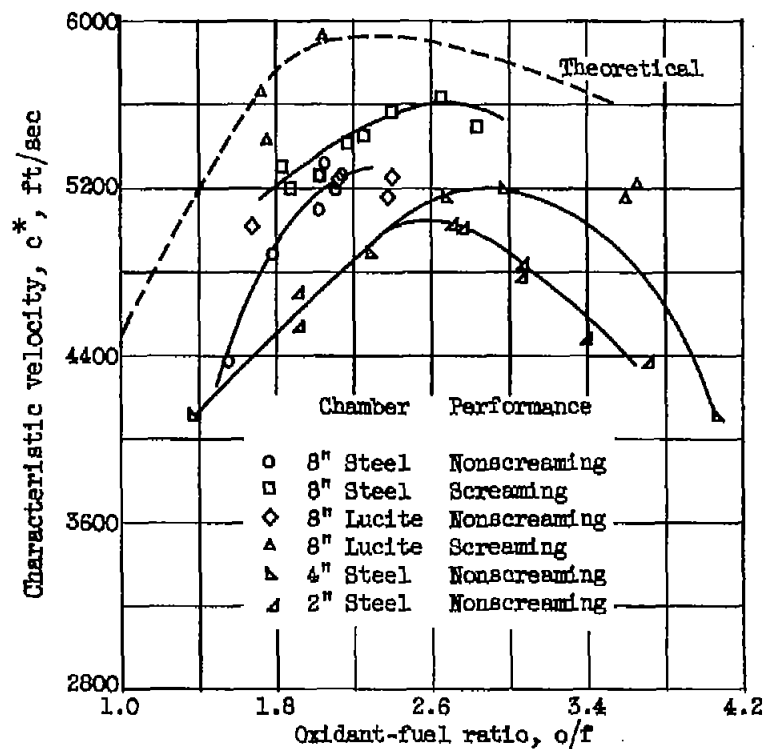


CD-4233



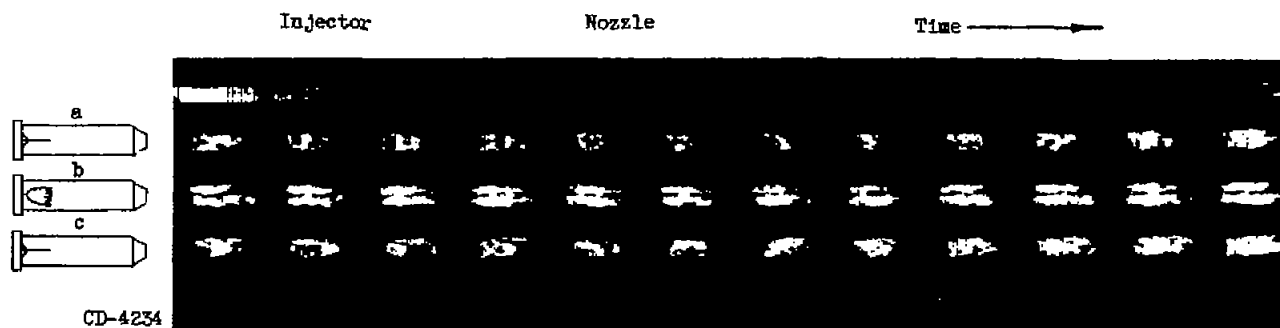
(a) Injector design and water-spray photograph.

Figure 9. - Impinging-jets long-stream-length injector for mixing before atomization.

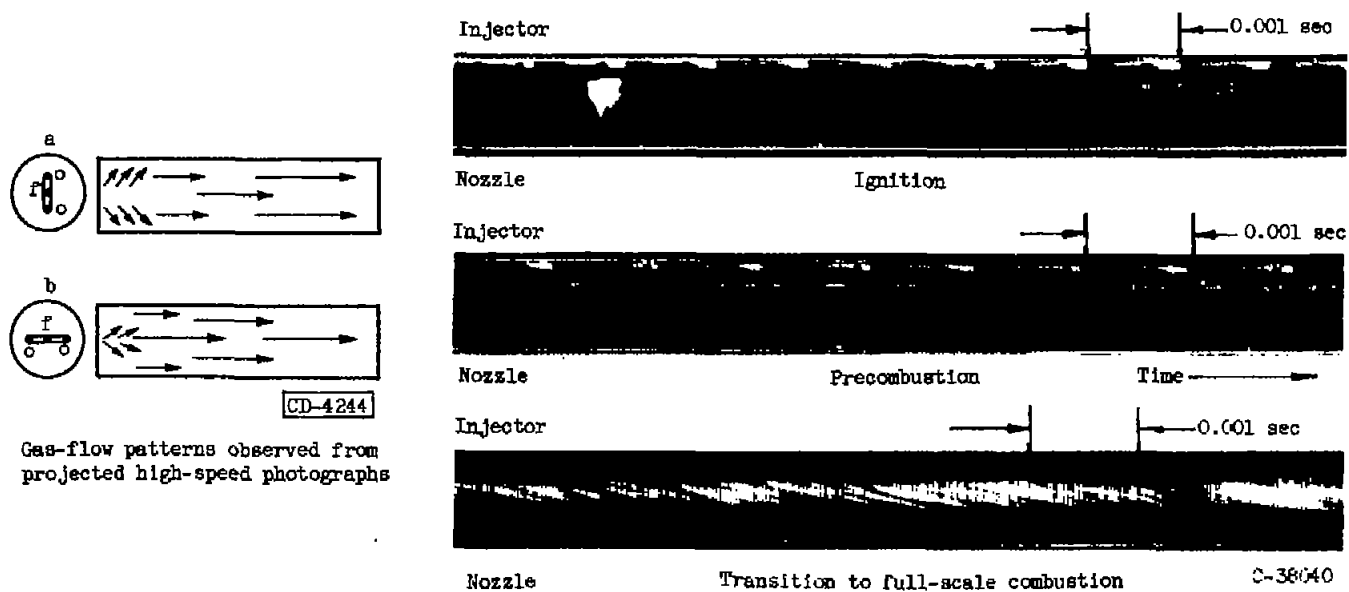


(b) Performance characteristics.

Figure 9. - Continued. Impinging-jets long-stream-length injector for mixing before atomization.



Enlarged 3000-frame-per-second photographs of combustion

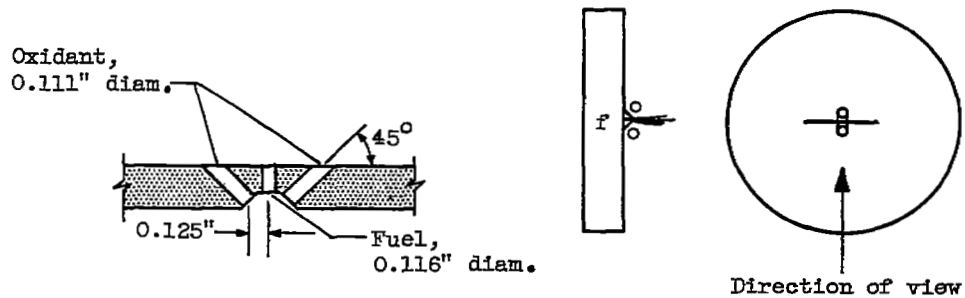


Streak photographs of ignition and starting

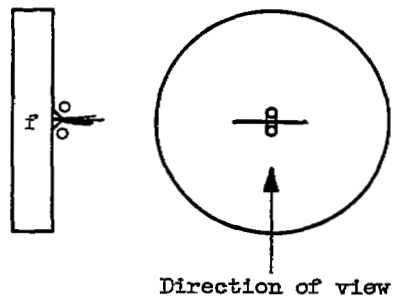
(c) Combustion photographs and flow patterns.

Figure 9. - Concluded. Impinging-jets long-stream-length injector for mixing before atomization.

3572



Injection method



Injection pattern

CD-4233

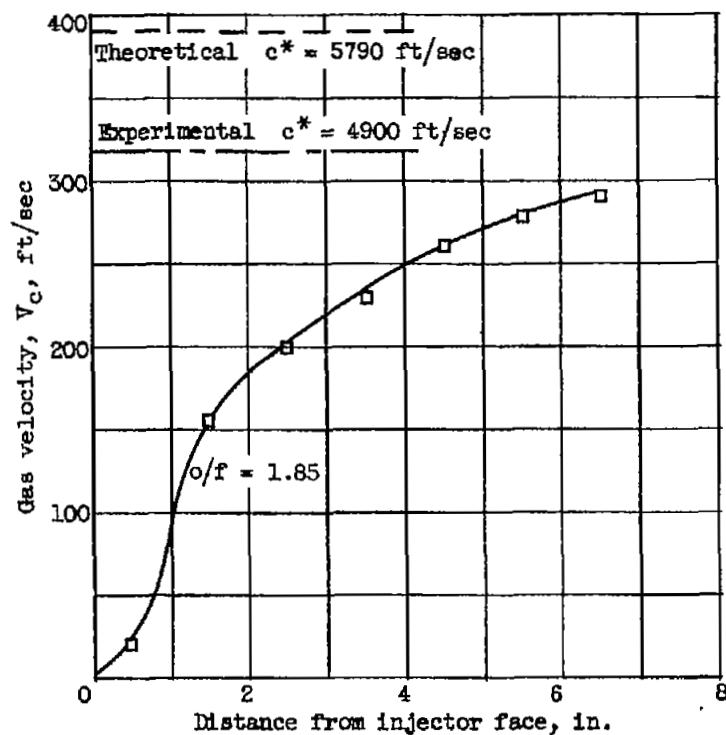
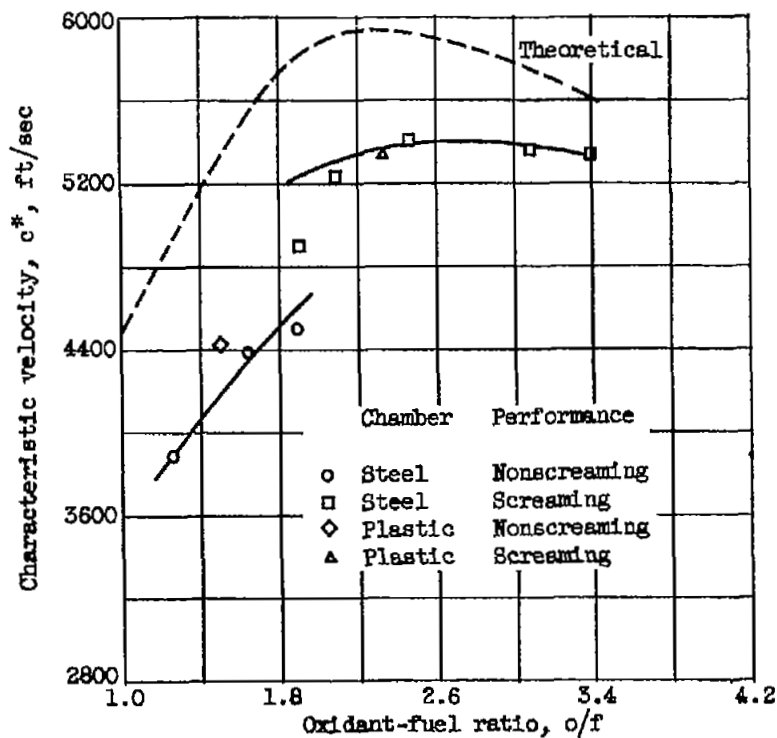
CU-6 back



Spray photograph

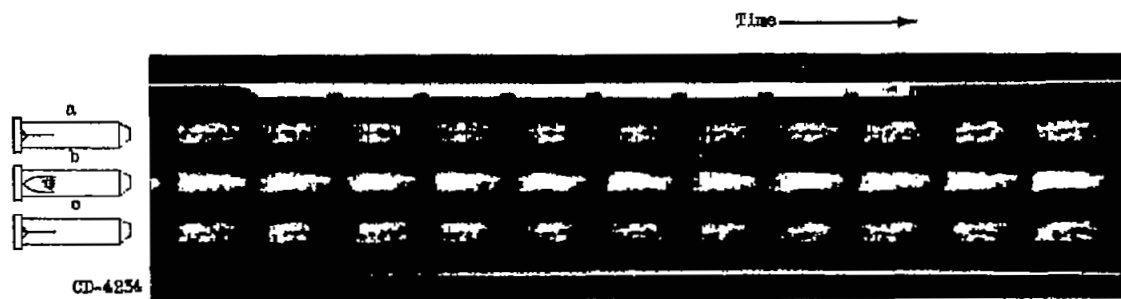
(a) Injector design and water-spray photograph.

Figure 10. - Impinging-jets surface-impinging injector for mixing before atomization.



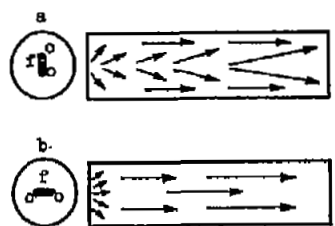
(b) Performance characteristics.

Figure 10. - Continued. Impinging-jets surface-impinging injector for mixing before atomization.



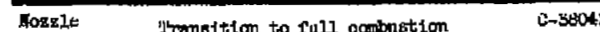
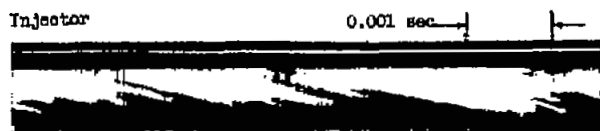
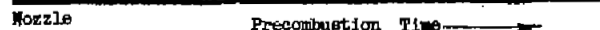
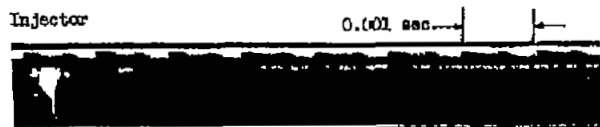
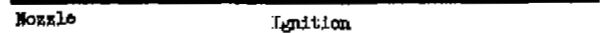
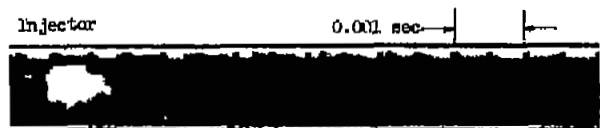
CD-4254

Enlarged 2000-frame-per-second photographs of combustion



Gas-flow patterns observed from projected high-speed photographs.

CD-4244

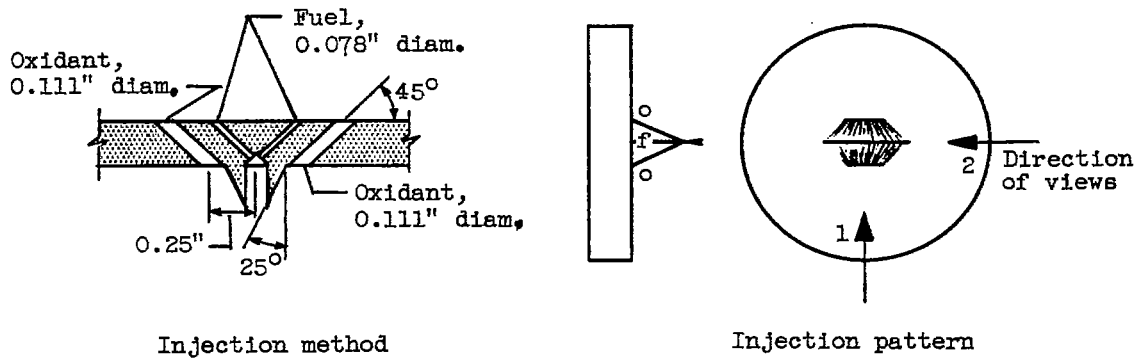


Streak photographs of ignition and starting

C-38042

(c) Combustion photographs and flow patterns.

Figure 10. - Concluded. Impinging-jets surface-impinging injector for mixing before atomization.



CD-4233



View 1

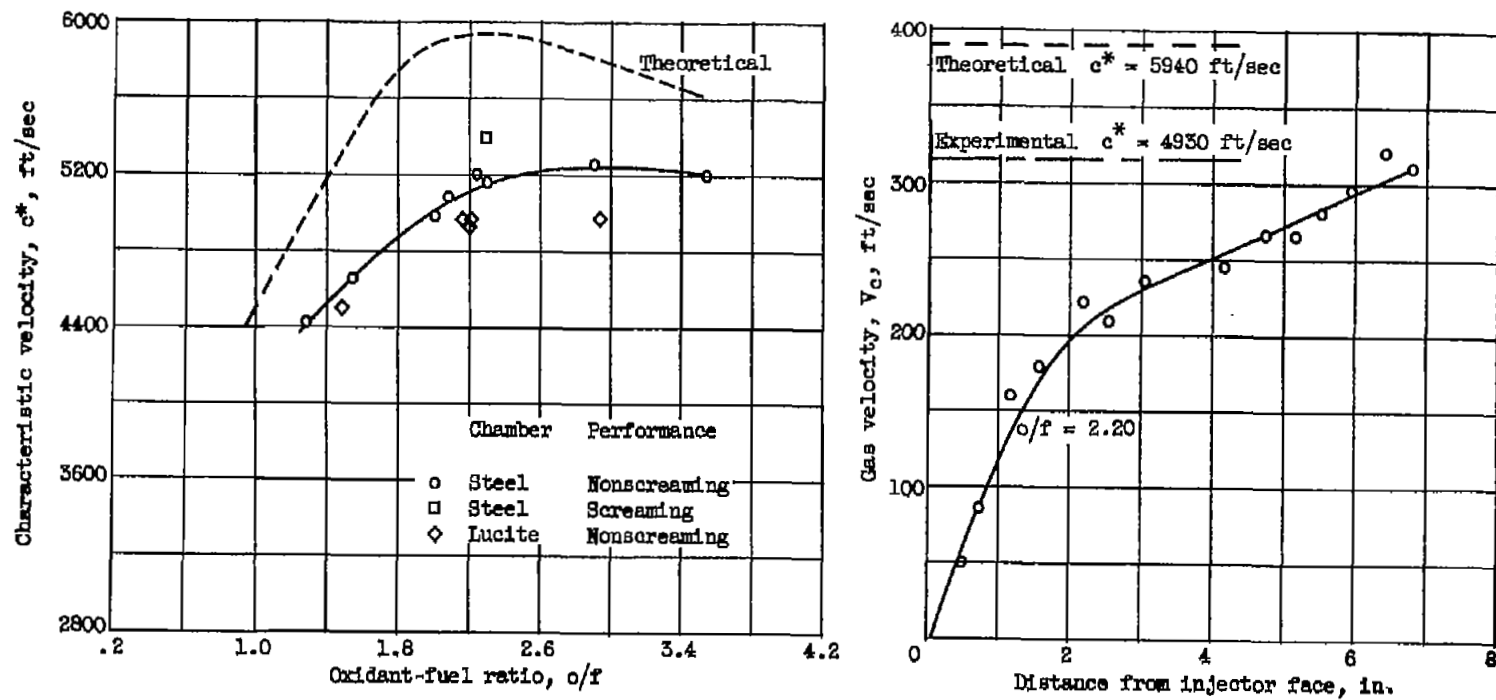


View 2

## Spray photographs

(a) Injector design and water-spray photographs.

Figure 11. - Impinging-sheets injector for mixing after atomization.

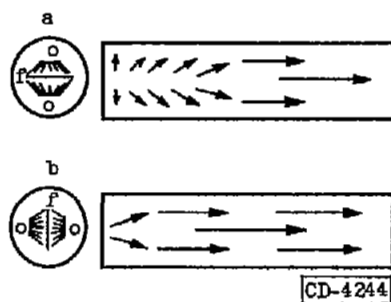


(b) Performance characteristics.

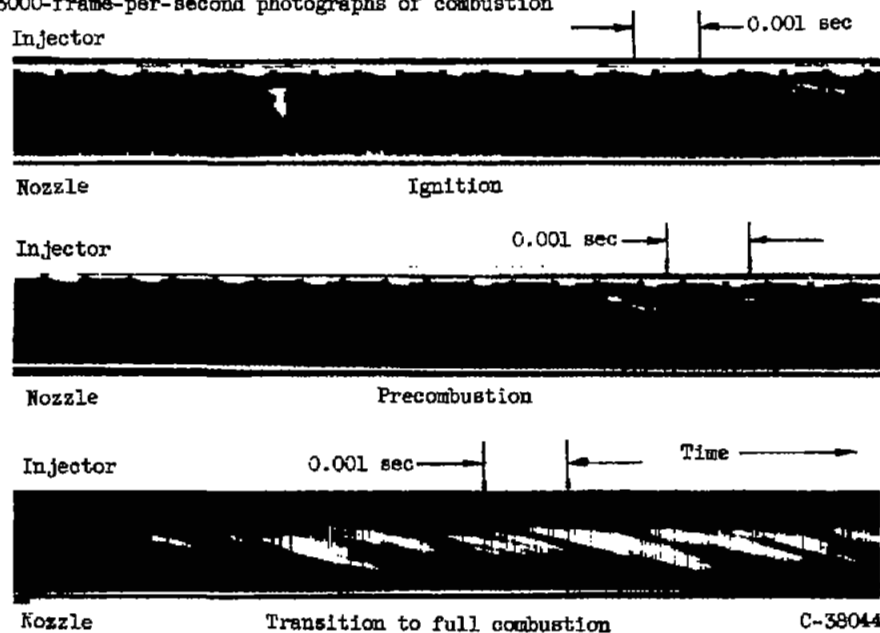
Figure 11. - Continued. Impinging-sheets injector for mixing after atomization.



Enlarged 3000-frames-per-second photographs of combustion



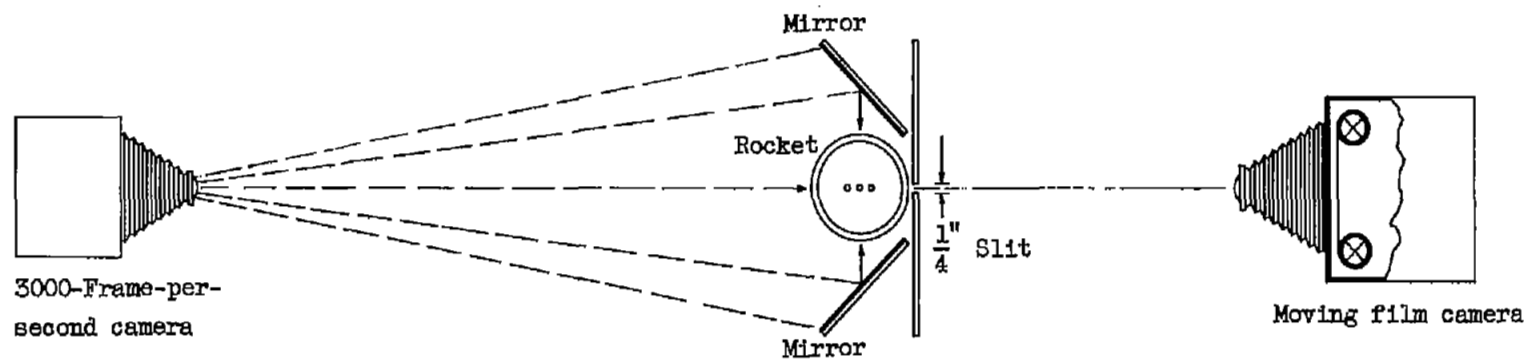
Gas-flow patterns observed from projected high-speed photographs



Streak photographs of ignition and starting

(c) Combustion photographs and flow patterns.

Figure 11. - Concluded. Impinging-sheets injector for mixing after atomization.



CD-3973

Figure 12. - Photographic arrangement for high-speed motion pictures and streak photographs of combustion.

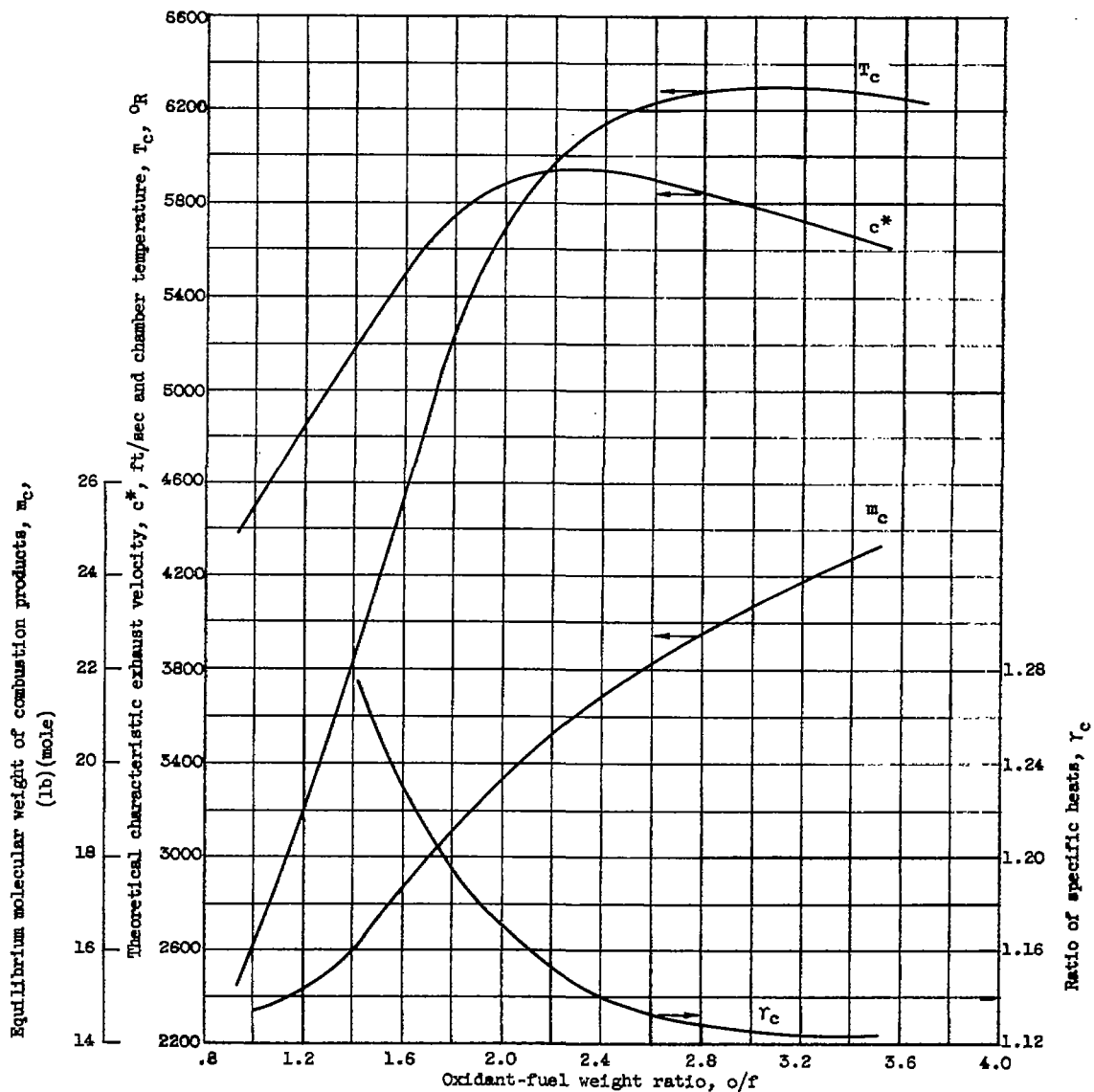
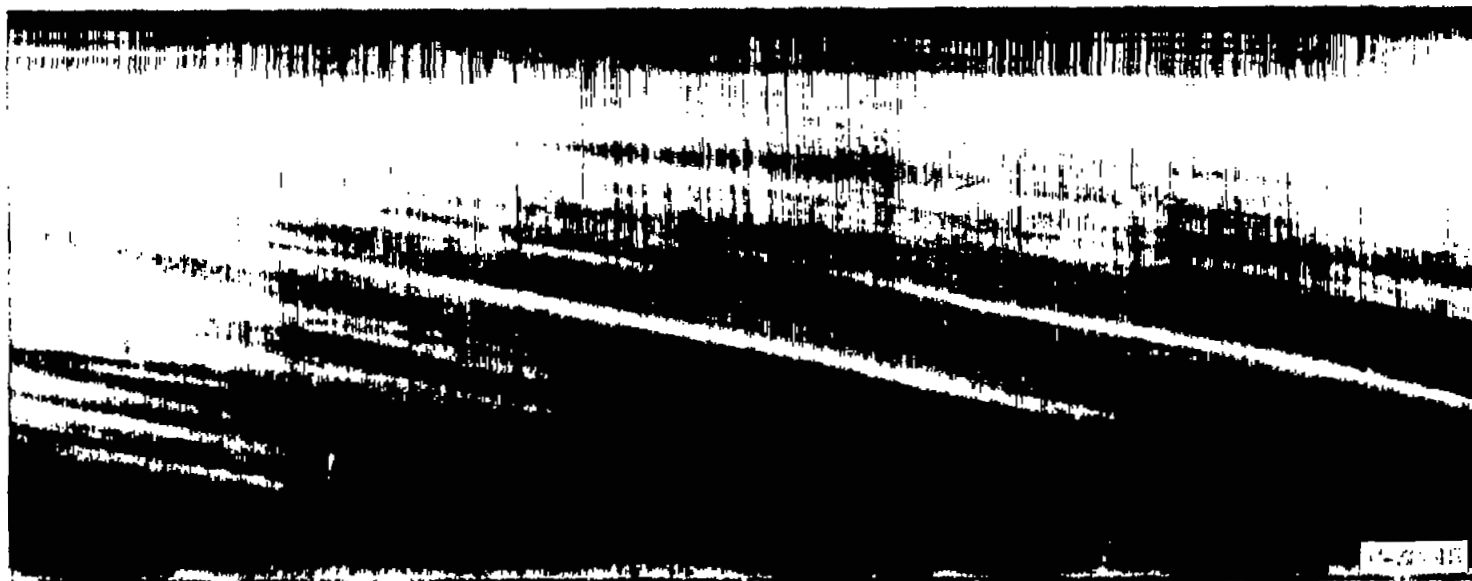
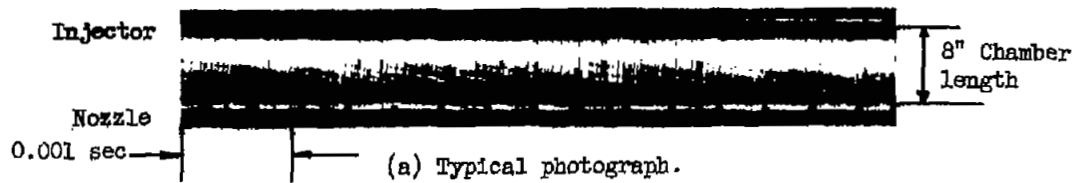


Figure 13. - Equilibrium properties of liquid oxygen - heptane propellant combination.



0.001 sec

(b) Enlarged portion of photograph.

Figure 14. - Streak photograph of rocket during smooth combustion.

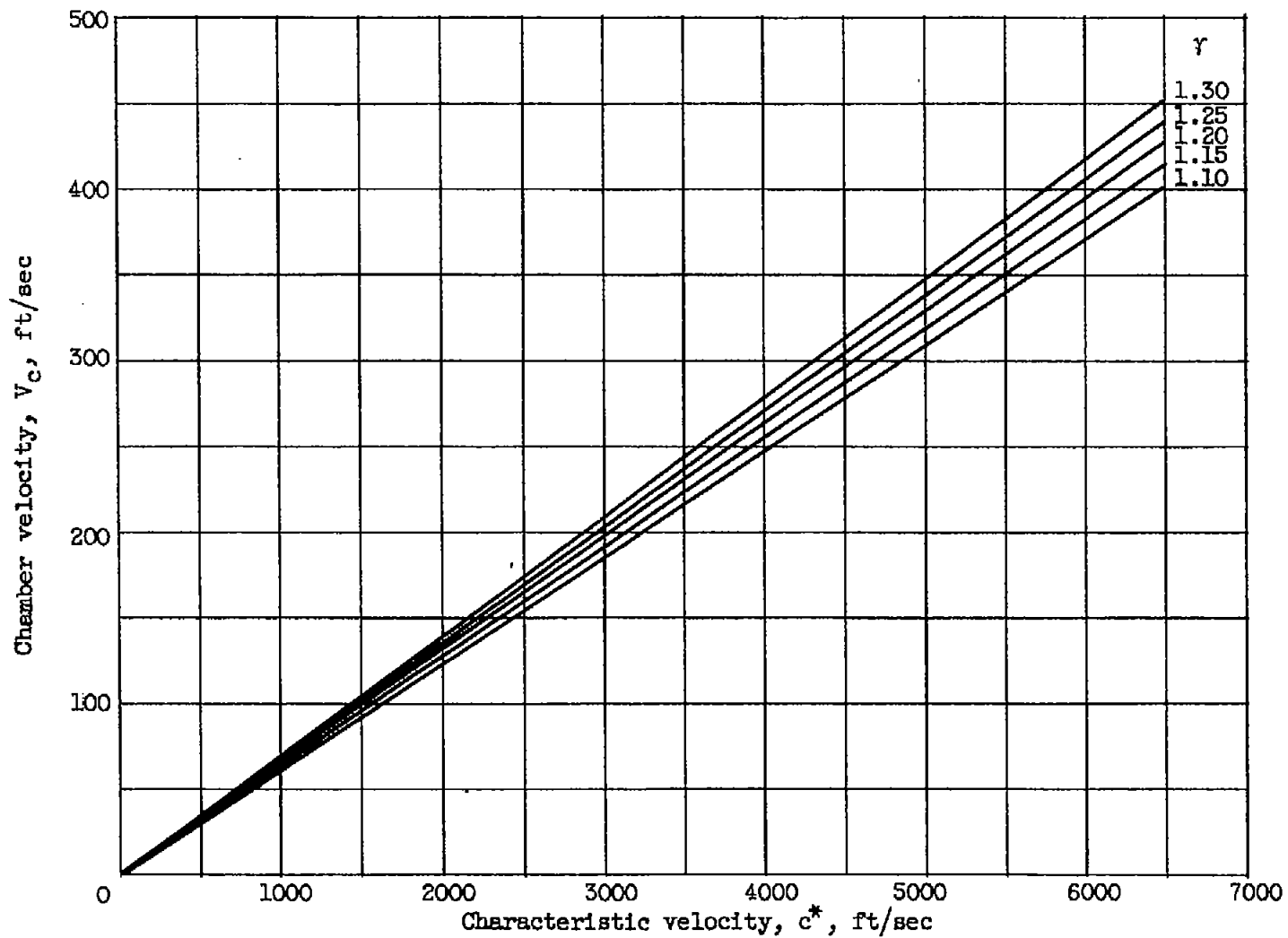
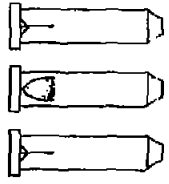
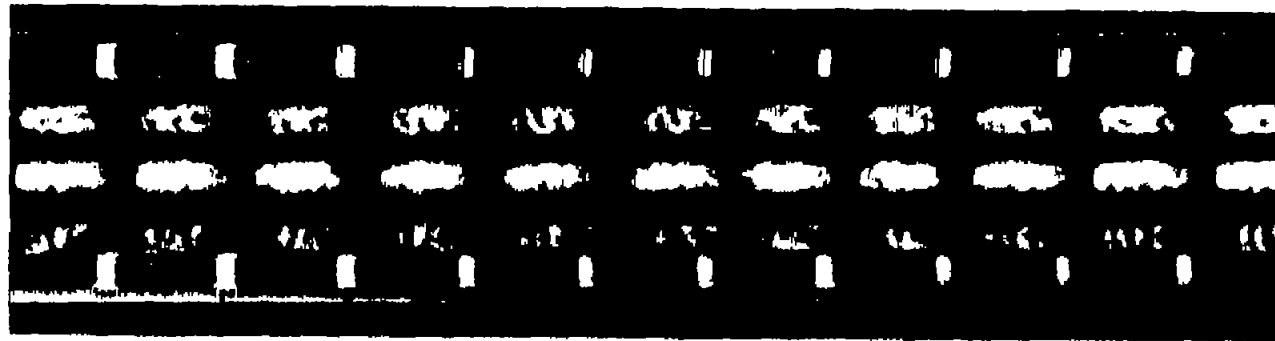


Figure 15. - Theoretical variation of characteristic velocity with chamber velocity with variable specific heat ratio. Contraction ratio, 6.41.



CD-4234



(a) Combustion instability. Motion pictures (3000-frame/sec); impinging-jet long-stream-length injector.

Time →

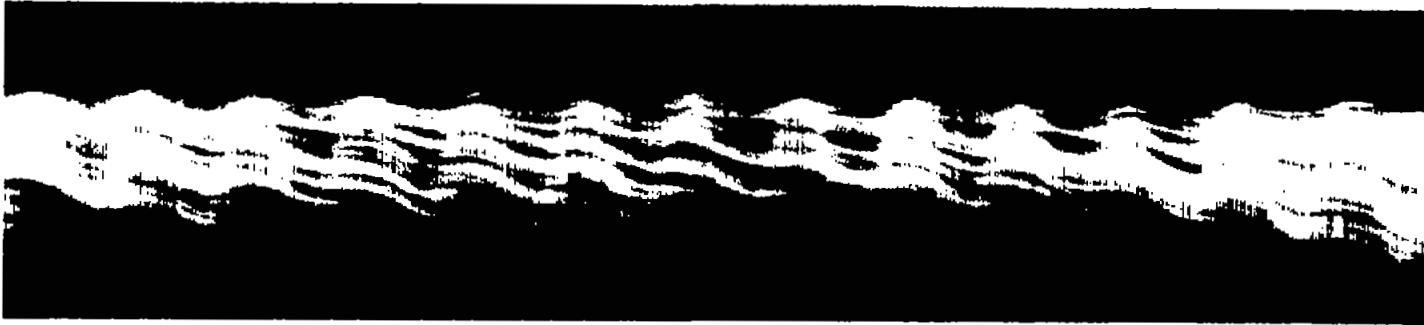
Injector



Nozzle

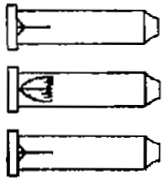
(b) Combustion instability. Slit photography; impinging-jet long-stream-length injector.

Figure 16. - Photographic description of combustion instability.



(c) Combustion instability. Streak photography; parallel oxidant-jet - fuel-sheet injector.

Injector



CD-4234



Nozzle

(d) Transition from stable to unstable combustion. Motion pictures (3000 frames/sec); impinging-jet long-stream-length injector.

Figure 16. - Concluded. Photographic description of combustion instability.

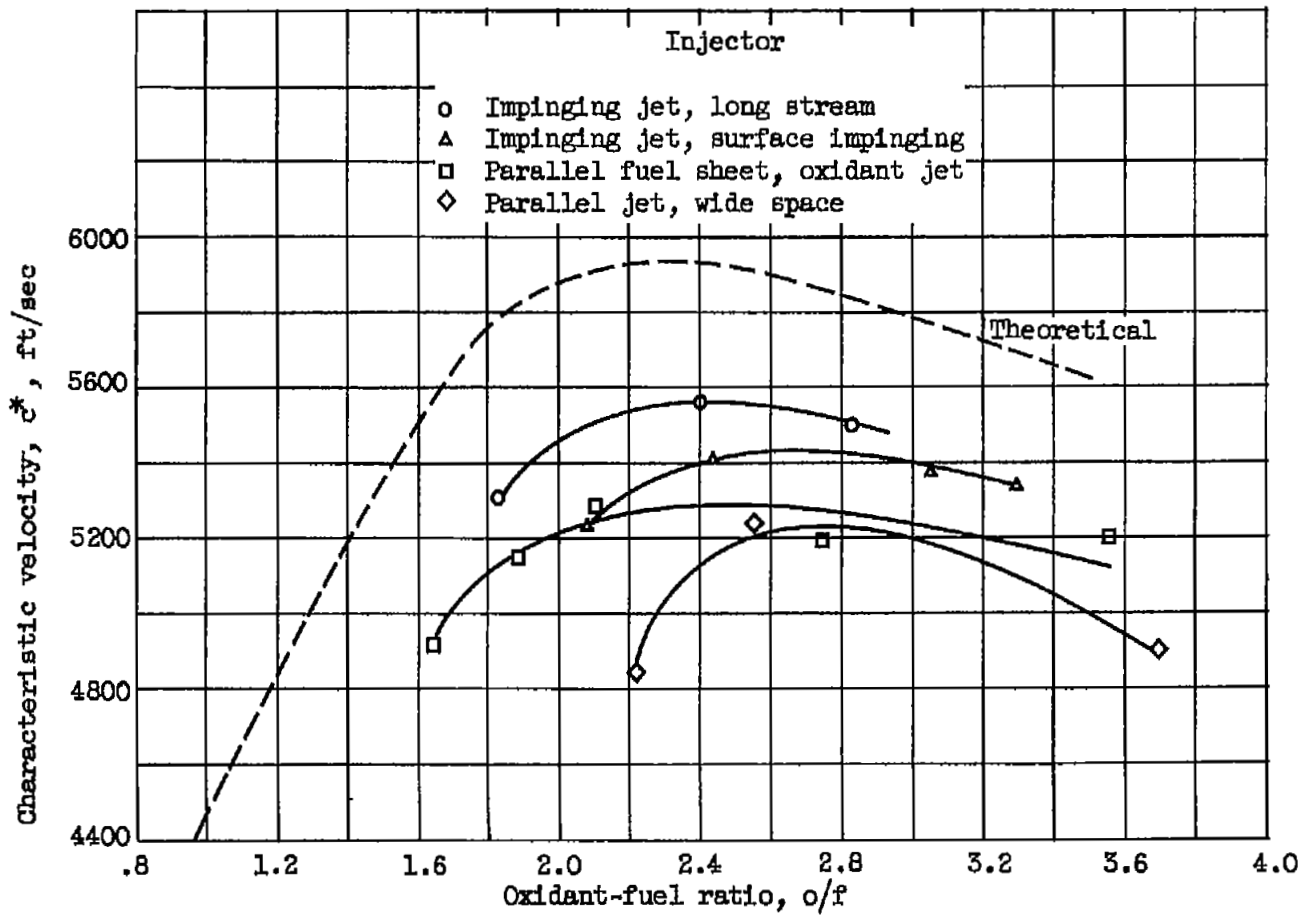


Figure 17. - Characteristic velocity performance of four injectors during screaming operation.

[REDACTED]



3 1176 01435 8197



1

1

1

[REDACTED]